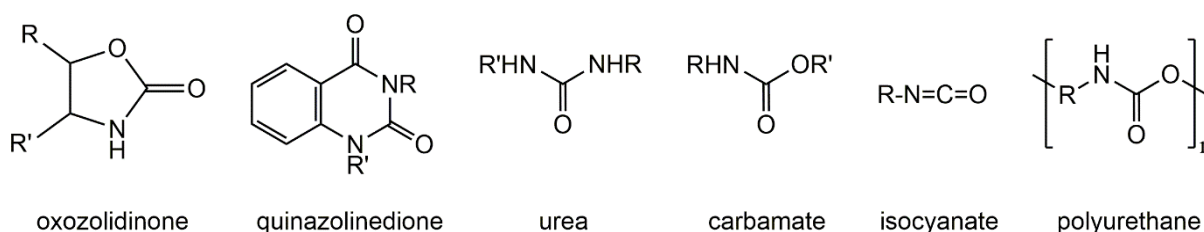




Ge, Sn, Pb), toward small molecules also aroused a growing interest [15,16]. In this context and based on our previous work in this field, we have recently reviewed molecular organotin compounds bearing hemi-carbonate and carbonate ligands and which result from the reactivity of tin precursors towards carbon dioxide [1]. In this second part, we continue to explore from a structural point of view the molecular derivatives of tin which result from the insertion of carbon dioxide into the Sn–X bonds (X = N, H, P). Thus, the formation and structures of carbamato, formato and phosphinoformato tin derivatives are successively described and discussed. The last chapter is devoted to metalcarboxylato tin complexes exhibiting a bridging CO<sub>2</sub> ligand. Although these latter compounds are not derived from the direct reactivity of tin precursors with carbon dioxide, we found appropriate to include them in this review. Regarding the general method used to carry out this inventory, the compounds described below were identified from the data available on the online portal of the Cambridge Structural Database (CSD) web interface (2017) [17]. In addition to the structural description, comparison tables including selections of structural and spectroscopic data are also displayed at the end of each section (Tables 1–8).

Among the useful chemicals with higher added-value which can be produced by the transformation of CO<sub>2</sub>, the derivatives involving C–N bonds occupy an important place, historically and economically. Thus, from 1922, the German Bosch-Meiser process allowed the industrial use of carbon dioxide (together with ammonia) as raw material for the synthesis of urea [(NH<sub>2</sub>)<sub>2</sub>CO]. It is still today the most important industrial chemical process in terms of CO<sub>2</sub> amounts converted (115 Mt) [18]. Since then, the use of carbon dioxide as C1 synthon has been extended to the synthesis of other types of nitrogen compounds such as oxazolidinones, quinazolidinones, ureas, carbamates, isocyanates and polyurethanes (Scheme 1). These molecules constitute intermediates and derivatives of great importance for the chemical, agrochemical and pharmaceutical industry. The domain was firstly reviewed by He et al. in 2012 [19], and recently updated by Song et al. [20] and then by Dalpazzo et al. [21], both in 2019. In most cases, the intervention of a catalytic precursor—organic or organometallic, is required to achieve the targeted product.

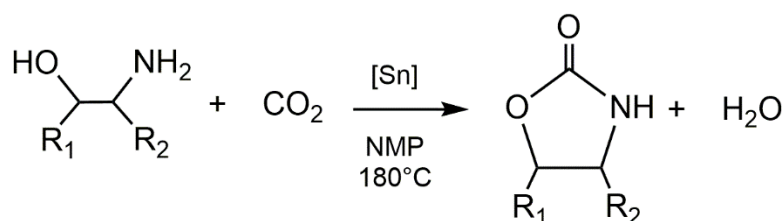


**Scheme 1.** Molecular representations of nitrogen-containing molecules accessible from CO<sub>2</sub> used as a C1 building block.

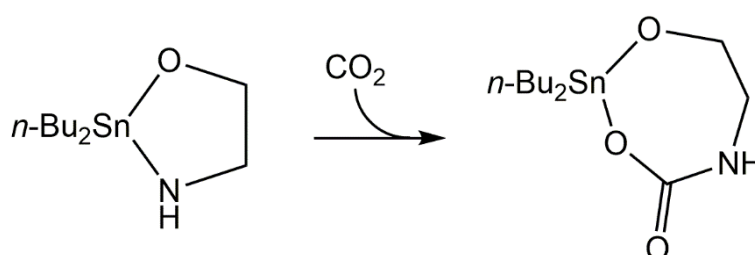
#### *Tin-Promoted Insertion Reaction of CO<sub>2</sub> into C–N Bonds*

Regarding more specifically the use of main group metals as catalytic species for the insertion of CO<sub>2</sub> into the C–N bond, the beneficial role of organotin compounds was regularly emphasized in the past, being the subject of several studies. In 2002, Tominaga and Sasaki found that di-*n*-butyltin oxide, *n*-Bu<sub>2</sub>SnO, was an effective catalyst for the dehydrating condensation of 1,2-aminoethanols with carbon dioxide to lead to the formation of 2-oxazolidinones [22] (Scheme 2). Reactions were carried out under 5 MPa of CO<sub>2</sub>, at 180 °C, for 16 h, in *N*-methyl-2-pyrrolidone (NMP) as solvent and gave satisfactory yields in the range of 53 to 94%. The use of NMP has been found to be more effective than the use of protic and non-polar solvents. From a mechanistic point of view, the authors proposed the formation of a seven-membered cyclic tin carbamate complex (Scheme 3) by the insertion of CO<sub>2</sub> into the Sn–N bond of a stanna-oxazolidine species and whose in-situ formation was supported by electrospray mass spectrometry. However, to our knowledge, such a species has not been yet structurally isolated. From this intermediate,

the intramolecular elimination of one molecule of 2-oxazolidinone was suggested to explain the regeneration of the starting complex,  $n\text{-Bu}_2\text{SnO}$ .

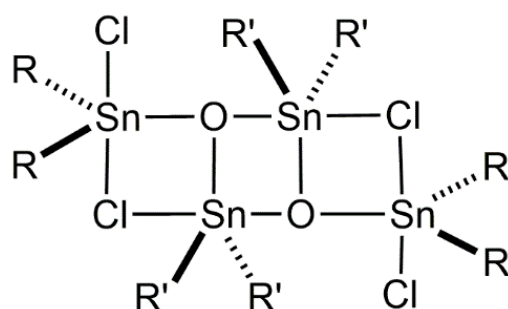


**Scheme 2.** Synthesis of 2-oxazolidinones from  $\text{CO}_2$  and 1,2-aminoalcohols catalyzed by  $n\text{-Bu}_2\text{SnO}$ , data from [22].



**Scheme 3.** Key step requiring the insertion of  $\text{CO}_2$  into the Sn–N bond of the stanna-oxazolidine species formed in situ, data from [22].

In 2013, Ghosh et al. revisited the previous reaction using chlorostannoxane derivatives, 1,3-dichloro-1,1,3,3-tetraalkyldistannoxanes (Scheme 4), as catalytic precursor, in methanol under 1.72 MPa of  $\text{CO}_2$  pressure and at 150 °C [23]. Chlorostannoxanes were selected because of (i) the presence of multi-active catalytic centers, and (ii) the ability to control Lewis acidity by changing the substituents on the metal centers. In comparison to the previous Tominaga's study using  $n\text{-Bu}_2\text{SnO}$  [22], an improvement of turnover numbers was recorded using chlorostannoxanes, from 9 to 138. Furthermore, it has been demonstrated that the activity of the catalytic precursors depends on the nature of the R and R' substituents, the  $n$ -butyl derivative (R and R' =  $n\text{-Bu}$ ) being the most efficient.

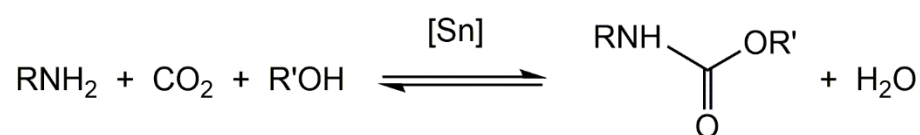


**Scheme 4.** Molecular representation of chlorostannoxane compounds used as tin precursors for the synthesis of 2-oxazolidinones by direct condensation of 2-aminoalcohols with carbon dioxide (R =  $n\text{-Bu}$ , Ph; R' =  $n\text{-Bu}$ , Ph), data from [23].

The direct synthesis of carbamates from carbon dioxide has also aroused renewed interest in the past two decades [24]. The state of the art was well established in 2003 by Calderazzo et al. [25] and recently updated by Marchetti et al. [26]. Indeed, carbamates can be viewed as a potential alternative to access to isocyanates, which are historically employed for the production of polyurethanes (PU). Industrially, isocyanates are produced by reacting primary amines with phosgene, but handling of this reactant is not without

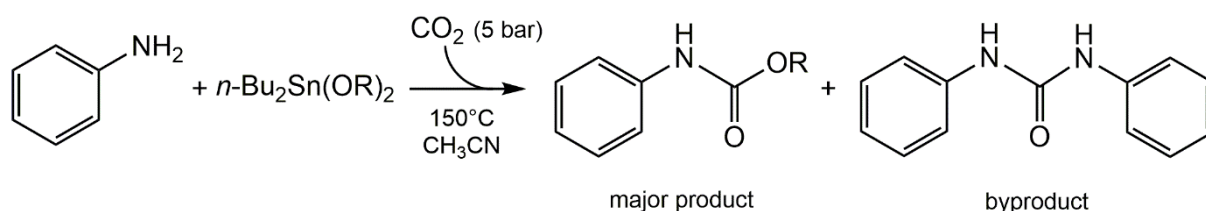
risks and requires drastic precautions. Therefore, the recent route based on the thermal decomposition of carbamates into isocyanates can be considered as a safer and greener synthetic pathway [27,28].

In the past, several groups investigated the action of organotins as catalyst precursors for the direct conversion of CO<sub>2</sub> into carbamates. In 2001, Sakakura et al. first published the synthesis of carbamates by reaction of amines and alcohols catalyzed by tin complexes (*n*-Bu<sub>2</sub>SnO and Me<sub>2</sub>SnCl<sub>2</sub>) [29] (Scheme 5). Optimal reaction conditions require a pressure of 30 MPa (300 bar) at 200 °C for 24 h. Moreover, the addition of acetals (2,2-diethoxy- or 2,2-dimethoxypropane) acting as a dehydrating agent significantly improves the conversion, and the increase in pressure promotes the urethane selectivity.



**Scheme 5.** Halogen-free process for the conversion of carbon dioxide to carbamates, data from [29].

In 2016, Choi et al. reported the synthesis of *N*-phenylcarbamates from CO<sub>2</sub> and aniline promoted by several di-*n*-butyltin dialkoxides: *n*-Bu<sub>2</sub>Sn(OMe)<sub>2</sub>, *n*-Bu<sub>2</sub>Sn(OEt)<sub>2</sub>, *n*-Bu<sub>2</sub>Sn(OPr-*n*)<sub>2</sub>, and *n*-Bu<sub>2</sub>Sn(OBu-*n*)<sub>2</sub> (Scheme 6) [30]. The best yield of *N*-phenylcarbamate (41%) was obtained under 5 MPa (5 bar) of CO<sub>2</sub> for 20 min at 150 °C using *n*-Bu<sub>2</sub>Sn(OMe)<sub>2</sub> as tin precursor. The catalytic activity changes depending on the nature of the alkoxide substituents linked to the tin atom [*n*-Bu<sub>2</sub>Sn(OMe)<sub>2</sub> > *n*-Bu<sub>2</sub>Sn(OPr-*n*)<sub>2</sub> > *n*-Bu<sub>2</sub>Sn(OEt)<sub>2</sub> > *n*-Bu<sub>2</sub>Sn(OBu-*n*)<sub>2</sub>]. *N,N'*-diphenylurea is formed as byproduct (4%). From a mechanistic point of view, the hemicarbonato tin complex, *n*-Bu<sub>2</sub>Sn(OMe)(OCO<sub>2</sub>Me), resulting from the reactivity of CO<sub>2</sub> with *n*-Bu<sub>2</sub>Sn(OMe)<sub>2</sub> [1,31], is claimed as the key intermediate of the reaction. In the case of reactions involving *n*-Bu<sub>2</sub>Sn(OBu-*n*)<sub>2</sub>, the authors also showed that the starting tin complex could be regenerated after the first catalytic run (by reacting with *n*-BuOH) and could thus be recycled without loss of activity.



**Scheme 6.** Tin-promoted synthesis of *N*-phenyl carbamate from aniline and carbon dioxide (R = Me, Et, *n*-Pr, and *n*-Bu), data from [30].

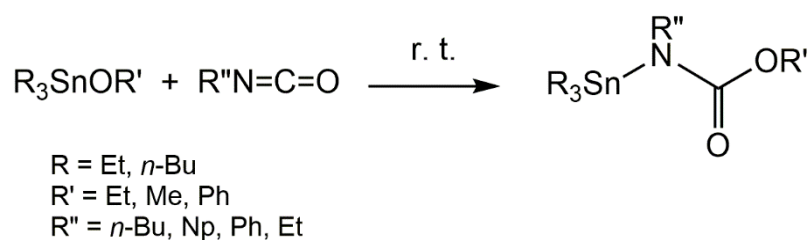
Concomitantly and supported by density functional theory (DFT) calculations, Schaub et al. confirmed that dialkyltin(IV) dialkoxides can be used as reagents for the synthesis of aromatic carbamates from aromatic amines and carbon dioxide [32]. The process takes place between 60 and 70 bar of pressure, at 135 °C and in pentane as solvent. A NMR yield of 92% was recorded for the synthesis of methyl phenylcarbamate from aniline using three molar equivalent of *n*-Bu<sub>2</sub>Sn(OMe)<sub>2</sub>. Neither methylaniline nor diphenylurea was chromatographically detected. Extension of the reaction conditions to the synthesis of diurethanes from 4,4'-methylenedianiline and 2,4-diaminotoluene was successful with yields of 60 and 77%, respectively. In the perspective of an industrial development, the authors have demonstrated the possibility of regenerating and re-using the dialkyltin(IV) dialkoxides, by using an excess of dimethylcarbonate. Shortly after, in a new study, the same group improved the reaction yield (up to 97%) by combining with dialkyltin oxide, used as a tin precursor, tetraalkyl orthosilicates, which promote the generation of dialkyltin(IV) dialkox-

ides [33]. This positive effect had been initially shown for the tin-promoted synthesis of organic carbonates from carbon dioxide and alcohols [34].

## 2. Carbamate Tin Complexes

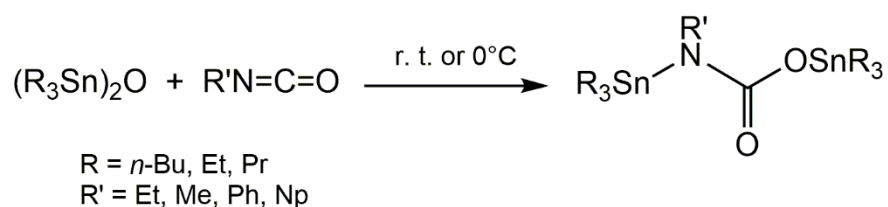
### 2.1. Early Works

Historically, the pioneering works on carbamates of tin derivatives dates back to the 1960s and are to be credited to A. J. Bloodworth and A. G. Davies who conducted extensive and fundamental investigations applying a systematic approach. From 1965, they described the synthesis of *N*-organo-*N*-trialkylstannylcarbamates resulting from the addition of trialkyltin alkoxides to isocyanates [35]. The reactions were reported as rapid and exothermic and taken place at room temperature (Scheme 7). Alkyl and aryl isocyanates exhibit a comparable reactivity.



**Scheme 7.** Formation of organo ester of *N*-organo-*N*-trialkylstannylcarbamic acid from trialkyltin alkoxides and isocyanates, data from [35].

Additionally in 1965, the study was then extended to bis(trialkyltin) oxides, which react exothermically with isocyanates to lead to trialkyltin *N*-trialkylstannylcarbamates (Scheme 8) [36].

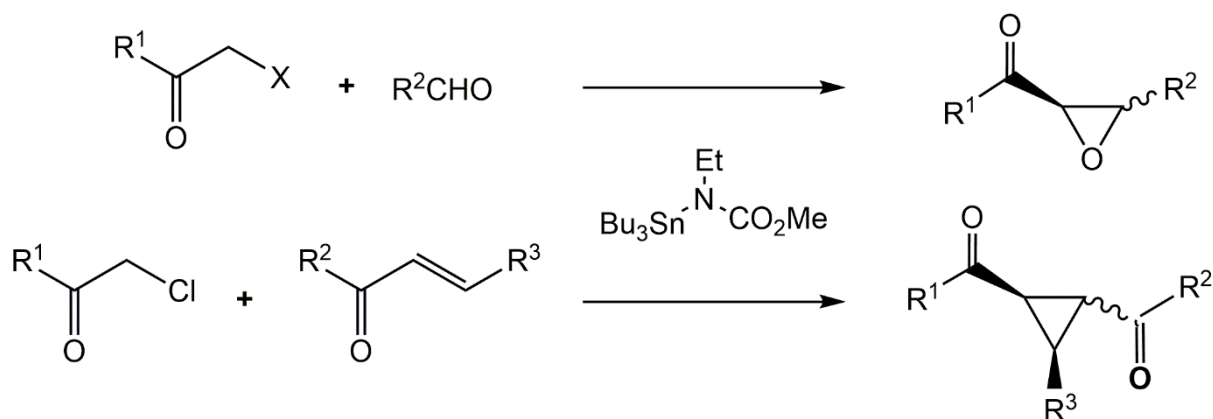


**Scheme 8.** Formation of trialkyltin ester of *N*-organo-*N*-trialkylstannylcarbamic acid from bis(trialkyltin) oxides and isocyanates, data from [36].

From a coordination point of view, the authors preferentially recommended the representation of the carbamate ligand as *N*-coordinated to tin, in amido form, but did not exclude an *O*-coordination, in imido form, via an interconversion process. Subsequently, this structural consideration was the subject of several subsequent works, involving other research groups, and based on studies carried out by  $^{119}\text{Sn}$  Mössbauer spectroscopy [37], as well as more recently by computational calculations [38].

### 2.2. Reactivity

In terms of reactivity, *N*-organo-*N*-trialkylstannylcarbamates have been also involved in various organic reactions. In their initial article [35], Bloodworth and Davies showed in particular their reactivity towards acetic anhydride, ethylamine and ethanol, which lead, according to a metathetical process, to the corresponding urethanes. In 1968, the same authors reported the decarboxylation of trialkyltin esters of *N*-organo-*N*-trialkylstannylcarbamic acids by isocyanates and isothiocyanates providing an alternative route to the synthesis of carbodi-imides [39]. In 1992 and then in 1993, Shibata et al. underlined the positive and efficient role of methyl ester of *N*-ethyl-*N*-tributylstannylcarbamic acid as promoter for the Darzens reaction [40] and the addition of Michael [41] (Scheme 9).



**Scheme 9.** Darzens-type reaction (top) and Michael addition (bottom) promoted by methyl ester of *N*-ethyl-*N*-tributylstannylcarbamic acid, data from [40,41].

### 2.3. X-Ray Crystal Structures

Regarding the solid-state characterization of metal carbamates by single-crystal X-ray diffraction, the area was first reviewed by Calderazzo et al. [25] and then recently updated by Marchetti et al. [26]. To date, numerous examples of metal carbamates have thus been isolated and characterized, demonstrating a rich coordination chemistry and highlighting a great diversity of structures. Herein, we will focus exclusively on X-ray structures involving tin moieties. To the best of our knowledge, six CSD depositions of carbamato tin complexes have been identified up to now (CSD entries and deposition numbers are reported in Table 1).

The first X-ray crystallographic investigation on a tin complex bearing a carbamato ligand was reported by Zakharov et al. in 1980, as part of studies on organotin isocyanate derivatives [42]. Thus, the Russian group characterized at the solid-state the structure of the trimethyltin(IV) ester of *N*-trimethylstannylcarbamic acids,  $\text{Me}_3\text{SnNHC(=O)-OSnMe}_3$  (**1**), which describes a polymeric arrangement displaying a zigzag one-dimensional infinite chain along the *c*-axis (Figure 1). The organization of **1** consists of  $\text{SnMe}_3$  moieties bridged by carbamate dianions. Two distinct sites of tin atoms are distinguished: (i) those located in the main chain exhibiting a trigonal bipyramidal geometry (TBP) whose equatorial plane is occupied by three methyl substituents and the apical positions by two oxygen atoms; (ii)  $\text{SnMe}_3$  pendant groups, connected to the main chain by nitrogen atoms ( $\text{Sn-N} = 2.04(2)$  Å) and positioned in a syndiotactic arrangement, and whose tin atoms exhibit a tetrahedral geometry. This type of architecture is comparable to the chain-like structures reported for the organotin(IV) selenite complexes,  $(\text{Me}_3\text{Sn})_2\text{SeO}_3 \cdot \text{H}_2\text{O}$  and  $(\text{Ph}_3\text{Sn})_2\text{SeO}_3$  [43], as well as for the organotin(IV) carbonato complexes,  $(\text{Me}_3\text{Sn})_2\text{CO}_3$  and  $(i\text{-Bu}_3\text{Sn})_2\text{CO}_3$  [44]. However, the authors pointed out that, despite the presence of a hydrogen atom on the nitrogen of carbamato groups, no hydrogen bonds are observed between the chains, which is explained by the proximity of bulky  $\text{Me}_3\text{Sn}$  groups. Moreover, we consider that compound **1** is the only example of an *N*-coordinated tin carbamate, structurally characterized to date.

Thereafter, with the aim of applications in heterogeneous catalysis, Calderazzo et al. reported the preparation of two *N,N*-dialkylcarbamato tin(IV) complexes,  $\text{Sn}(\text{O}_2\text{CNi-Pr}_2)_4$  (**2**) and  $\text{Sn}(\text{O}_2\text{CNEt}_2)_4$  (**3**), which were used as precursors for the chemical implantation of metal cations on a silica support [45]. The grafting method consisted of promoting reactivity of *N,N*-dialkylcarbamates with silanol groups of silica. Compounds **2** and **3** were synthesized by treating anhydrous Sn(IV) chloride with diethylamine and di-*iso*-propylamine, respectively, in toluene at room temperature, under atmospheric pressure of carbon dioxide (Scheme 10). Yields higher than 90% are reported.

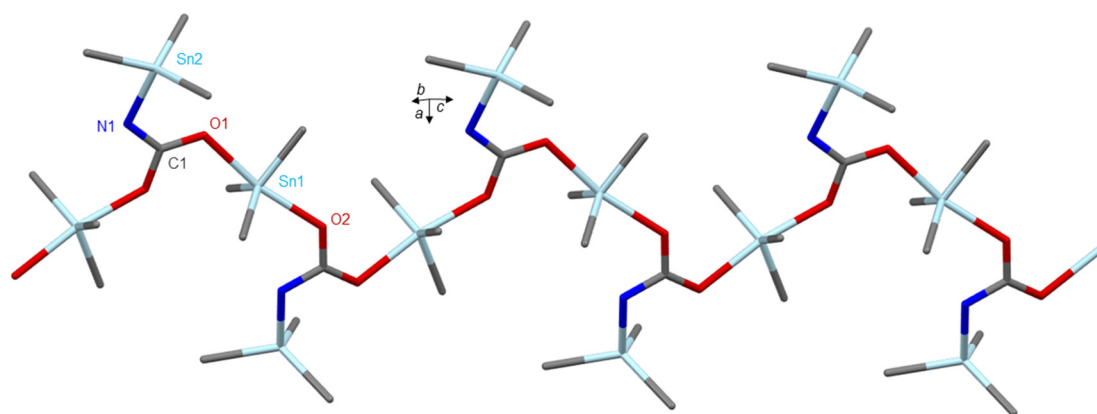
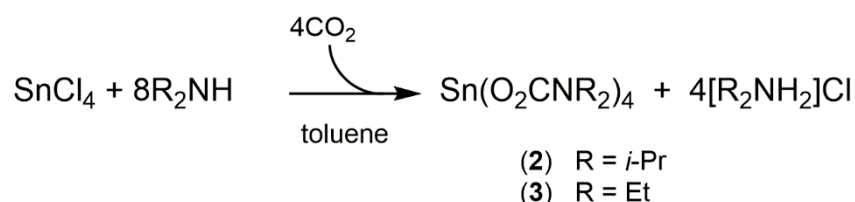
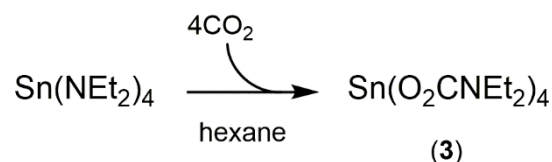


**Figure 1.** Molecular structure of **1**, adapted from [42] (MERCURY view). Hydrogen atoms are omitted for clarity (Sn light blue, O red, N dark blue, C grey).



**Scheme 10.** Reaction scheme leading to Compounds **2** and **3**, data from [45].

Recrystallized from heptane, suitable single crystals of **2** were analyzed by X-ray diffraction leading to the resolution of the crystallographic structure. In 2002, in the frame of metal-organic chemical vapor deposition (MOCVD) investigations, Molloy et al. described a new synthetic route to **3**, starting from a solution of tetrakis(*N,N*-diethylamino)tin(IV) complex in hexane that was bubbled with carbon dioxide (Scheme 11) [46].



**Scheme 11.** Alternative route leading to compound **3**, data from [46].

X-ray structures of **2** and **3** revealed comparable mononuclear molecules. In both compounds, the tin atom is eight-coordinated by four chelating *N,N*-dialkylcarbamato ligands, which are exclusively *O*-donor (Figure 2). For **3**, the authors suggest that the geometry can be viewed as a distorted square antiprism. From a spectroscopic point of view, similar  $^{119}\text{Sn}$  NMR chemical shifts were also recorded for **2** and **3**, at  $-920.8$  and  $-930.0$  ppm, respectively (Table 2). In  $^{13}\text{C}$  NMR, the carbamato carbons show one resonance at  $164.9$  ppm for **2**, and  $166.2$  ppm for **3**. In the case of **2**, CP/MAS  $^{13}\text{C}$  NMR measurements confirm the chemical shift recorded in solution. A thermogravimetric analysis was also carried out on **3** showing a continuous weight loss between room temperature and  $300$  °C (and resulting in the recovery of  $\text{SnO}_2$  as final residue). Beyond their interest as precursors for the deposition of tin oxide films [4,5], tin tetracarbamates were also used as versatile reactants for various organometallic and organic syntheses leading to alkoxytannanes [47], tetraalkynyltannanes [48] (Scheme 12), and *O*-silylurethanes [49].

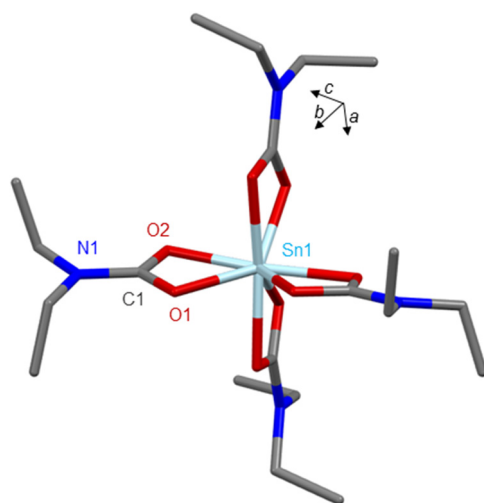
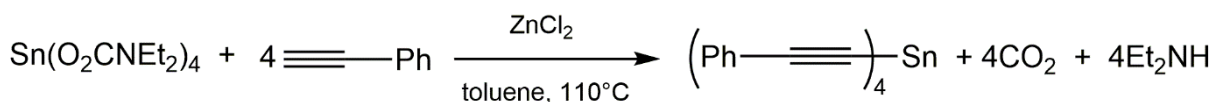
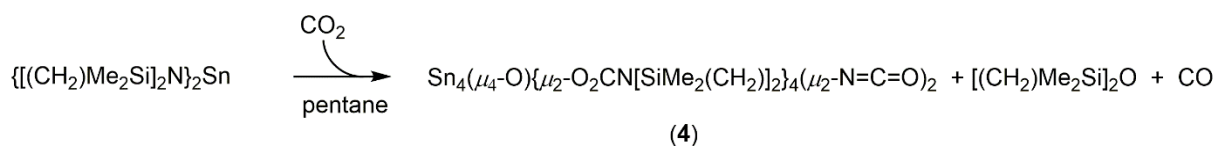


**Figure 2.** Molecular structure of **3**, adapted from [46] (MERCURY view). Hydrogen atoms are omitted for clarity (Sn light blue, O red, N dark blue, C grey).



**Scheme 12.** Reaction of tetrakis(*N,N*-diethylcarbamato)tin(IV) with phenylacetylene leading to tetra(phenylethynyl)tin, data from [47].

In 2010, Kemp et al. reported the reactivity of bis(2,2,5,5-tetramethyl-2,5-disila-1-azacyclopent-1-yl)tin toward  $\text{CO}_2$  leading to a silyl-substituted carbamate of tin(II) [50]. The exposure of  $\{[(\text{CH}_2)\text{Me}_2\text{Si}]_2\text{N}\}_2\text{Sn}$  in solution in pentane under 60 psig of  $\text{CO}_2$  (4 bar) at room temperature causes a rapid reaction involving a color change from red-orange to yellow. In parallel, GC–MS investigations on the reaction medium have shown the co-formation of carbon monoxide and the cyclic ether 2,2,5,5-tetramethyl-2,5-disila-1-oxacyclopentane,  $[(\text{CH}_2)\text{Me}_2\text{Si}]_2\text{O}$  (Scheme 13).  $\text{Sn}_4(\mu_4\text{-O})\{\mu_2\text{-O}_2\text{CN}[\text{SiMe}_2(\text{CH}_2)_2\}_4(\mu_2\text{-N}=\text{C}=\text{O})_2$  (**4**) was isolated as single crystals and analyzed by X-ray diffraction analysis. The unprecedented structure of **4** can be described as a tetranuclear tin cluster based on a  $[\mu_4\text{-O}]\text{Sn}_4$  core and including in periphery two bridging  $-\text{N}=\text{C}=\text{O}$  isocyanates and four bridging  $-\text{O}_2\text{CN}[\text{SiMe}_2(\text{CH}_2)_2]$  carbamate ligands (Figure 3). The presence of the central atom  $\mu_4\text{-O}$  was explained as resulting from the cleavage of  $\text{CO}_2$  and not from  $\text{O}_2$  or  $\text{H}_2\text{O}$ . Furthermore, the reaction of  $\{[(\text{CH}_2)\text{Me}_2\text{Si}]_2\text{N}\}_2\text{Sn}$  was also envisaged with  $\text{OCS}$  and  $\text{CS}_2$  leading, respectively, to an insoluble polymeric material and to a trinuclear cluster based on the coordination of three  $\{[(\text{CH}_2)\text{Me}_2\text{Si}]_2\text{N}\}_2\text{Sn}$  moieties by one  $\text{CS}_2$  molecule acting as  $\mu_3$  ligand. Previously, during the 1990s, Sita et al. explored already the reactivity of Ge and Sn complexes of silyl-containing amides toward carbon dioxide [51]. In particular, they focused on the reaction involving  $[(\text{Me}_3\text{Si})_2\text{N}]_2\text{Sn}$  with  $\text{CO}_2$ , which led to the isolation of the dimeric bisalkoxide complex,  $[\text{Sn}(\text{OSiMe}_3)_2]_2$ . However, in this case and compared to the Kemp's report, the tin carbamate is not stable but leads to the formation of  $[\text{Sn}(\text{OSiMe}_3)_2]_2$ , trimethylsilyl isocyanate, and 1,3-bis(trimethylsilyl)carbodiimide, respectively, according to a ligand metathesis process.



**Scheme 13.** Reaction scheme leading to Compound **4**, data from [50].

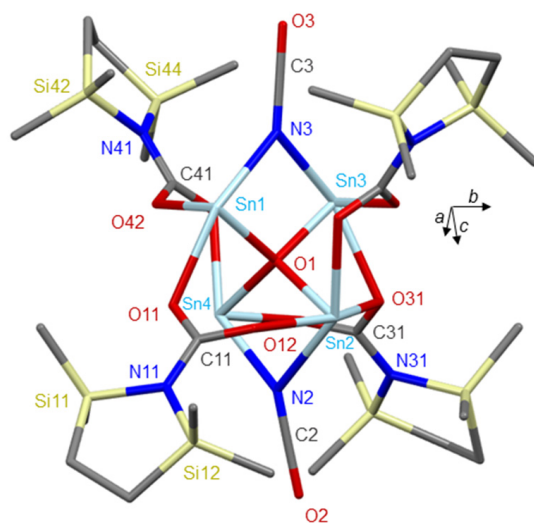
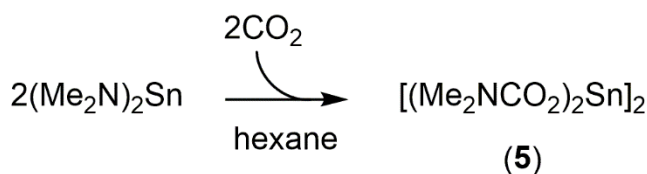


**Figure 3.** Molecular structure of **4**, adapted from [50] (MERCURY view). Hydrogen atoms are omitted for clarity (Sn light blue, O red, N dark blue, C grey, Si light yellow).

In 2011, continuing their study on the reactivity of silyl-substituted tin(II) amides towards heteroallenes, Kemp et al. reported the interaction of  $\text{CO}_2$ ,  $\text{OCS}$  and  $\text{CS}_2$  with  $(\text{Me}_2\text{N})_2\text{Sn}$  leading to the formation of insertion products characterized as bis(*N,N*-dimethylcarbamato)tin(II), bis(*N,N*-dimethylthiocarbamato)tin(II), and bis(*N,N*-dimethyldithiocarbamato)tin(II), respectively [52]. Thus,  $(\text{Me}_2\text{N})_2\text{Sn}$  in hexane solution reacts quickly with carbon dioxide, at room temperature and under atmospheric pressure, to give with a yield almost quantitative, the new complex  $[(\text{Me}_2\text{NCO}_2)_2\text{Sn}]_2$  (**5**) (Scheme 14). The authors describe the reaction as exothermic. In the solid-state, compound **5** is organized as a dimer involving two types of carbamato ligands: bridging and terminally ( $\eta^2$ -chelating) coordinated to Sn. From a supramolecular point of view, the existence of intermolecular interactions  $\text{Sn}\cdots\text{O}$  [2.8499(18) Å] between neighboring dimers and involving one oxygen atom of terminal carbamato ligands, leads to the propagation of a polymer chain (Figure 4). The coordination geometry of tin atoms can be viewed as a highly distorted trigonal bipyramid. In solution, the  $^{119}\text{Sn}$  NMR spectrum exhibits only one resonance at  $\delta$  -613 ppm. In the  $^{13}\text{C}$   $\{^1\text{H}\}$  NMR spectrum, the carbamato carbon also displays only one signal, not making it possible to differentiate the bridging and terminal modes highlighted in crystals of **5**.



**Scheme 14.** Reaction scheme leading to Compound **5**, data from [52].

To our knowledge, the latest tin carbamate structure resolved to date by X-ray diffraction is to be credited to Fulton et al., who published in 2011, the reactivity of  $\beta$ -diketiminato tin derivatives with carbon dioxide [53].  $[\text{HC}\{(\text{Me})\text{CN}(2,6\text{-}i\text{-Pr}_2\text{C}_6\text{H}_3)\}_2]\text{SnNi-Pr}_2$  and  $[\text{HC}\{(\text{Me})\text{CN}(2,6\text{-}i\text{-Pr}_2\text{C}_6\text{H}_3)\}_2]\text{SnNH}(2,6\text{-}i\text{-Pr}_2\text{C}_6\text{H}_3)$ , dissolved in toluene, react with  $\text{CO}_2$  (1 atm) at room temperature yielding to the corresponding carbamato tin(II) complexes,  $[\text{HC}\{(\text{Me})\text{CN}(2,6\text{-}i\text{-Pr}_2\text{C}_6\text{H}_3)\}_2]\text{SnOC}(\text{O})\text{Ni-Pr}_2$  (**6**) and  $[\text{HC}\{(\text{Me})\text{CN}(2,6\text{-}i\text{-Pr}_2\text{C}_6\text{H}_3)\}_2]\text{SnOC}(\text{O})\text{NH}(2,6\text{-}i\text{-Pr}_2\text{C}_6\text{H}_3)$  (**7**), respectively (Scheme 15). In the solid-state, **6** consists of a mononuclear complex describing a trigonal pyramidal arrangement of the ligands around the tin atom and in an *endo* configuration. The carbamate moiety is terminally *O*-bonded to Sn [ $\text{Sn}-\text{O} = 2.1346(16)$  Å] and its orientation can be viewed almost perpendicular to the NCCCN plane of the  $\beta$ -diketiminato ligand (Figure 5). This mode of coordination is

unusual for carbamates and is similar to that observed in the case of hemicarbonato derivatives [1]. The X-ray structure of complex 7 has not been reported but the spectroscopic data are very similar to 6 (Table 2) and the authors mention that for both compounds, the insertion reaction is irreversible, even under reduced pressure.

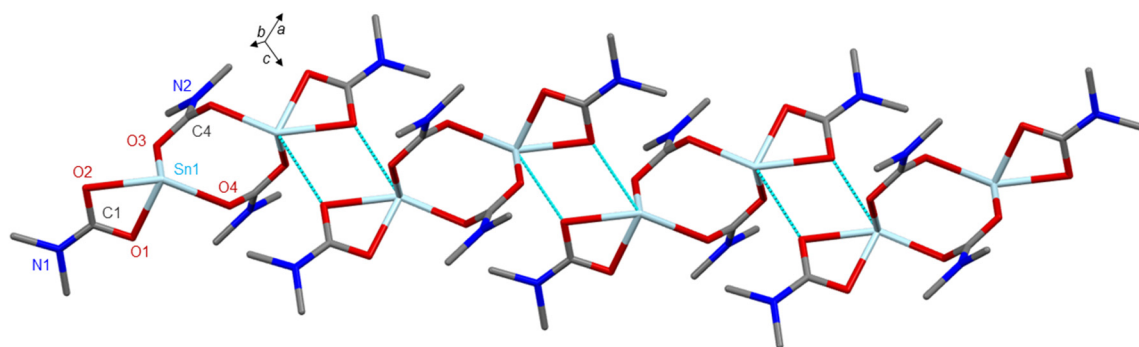
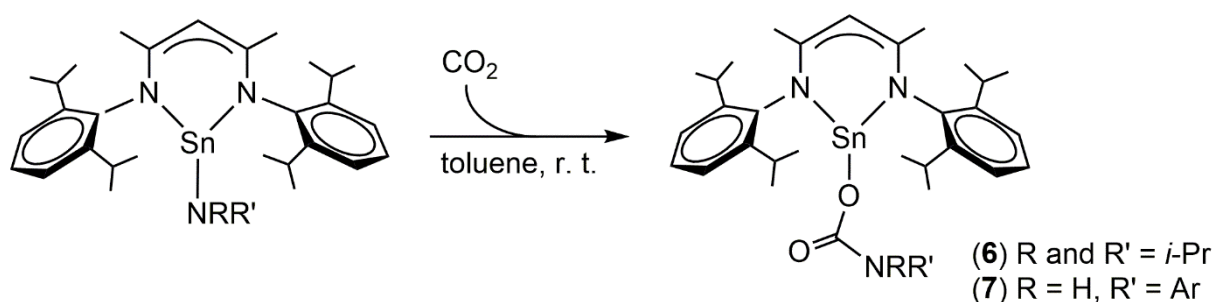


**Figure 4.** Molecular structure of 5, adapted from [52] (MERCURY view). Hydrogen atoms are omitted for clarity (Sn light blue, O red, N dark blue, C grey). Intermolecular hydrogen bonds are shown by cyan dash lines.



**Scheme 15.** Reaction scheme leading to Compounds 6 and 7, data from [53].

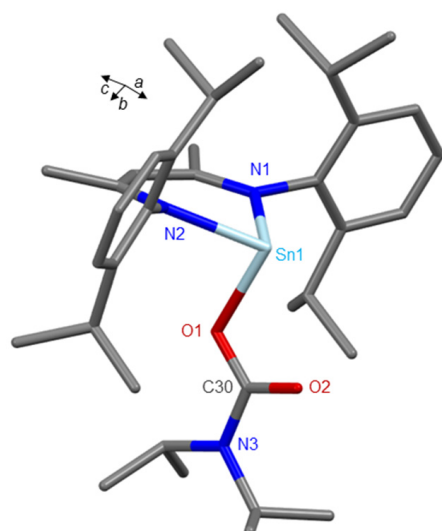


**Figure 5.** Molecular structure of 6, adapted from [53] (MERCURY view). Hydrogen atoms are omitted for clarity (Sn light blue, O red, N dark blue, C grey).

**Table 1.** Comparison of selected structural parameters found in carbamates of organotin complexes.

Compounds	Sn–O(C) (Å)	Sn–N(C) (Å)	C–O(Sn) (Å)	C=O (Å)	N–C(O <sub>2</sub> ) (Å)	O–C–O (deg)	N–C–O (deg)	CSD Entry Deposition Number	Ref.
Me <sub>3</sub> SnNHC(=O)–OSnMe <sub>3</sub> (1)	2.23(2) 2.24(2)	2.04(2)	1.27(4) 1.30(3)	na	1.35(4)	126(3)	120(2) 114(3)	MESNCB1211377	[42]
Sn(O <sub>2</sub> CNi-Pr <sub>2</sub> ) <sub>4</sub> (2)	2.146(5) 2.217(4) 2.136(5) 2.195(4) 2.198(4) 2.135(5) 2.219(4) 2.126(5)	na	1.283(7) 1.276(8) 1.279(7) 1.260(8) 1.268(8) 1.269(7) 1.275(8) 1.282(7)	na	1.33(1) 1.352(9) 1.34(1) 1.333(8)	117.7(6) 117.3(6) 116.1(6) 117.2(6)	119.9(6) 122.4(6) 122.9(6) 119.7(6) 120.6(6) 122.2(6) 116.1(6) 121.2(6)	MULPUE 196069	[45]
Sn(O <sub>2</sub> CNEt <sub>2</sub> ) <sub>4</sub> (3)	2.156(1) 2.209(1) 2.163(1) 2.196(1)	na	1.292(2) 1.277(2) 1.298(2) 1.276(2)	na	1.338(2) 1.331(2)	117.0(1) 116.6(1)	121.5(2) 121.7(1) 121.7(2)	UGOZUL 196788	[46]
Sn <sub>4</sub> (μ <sub>4</sub> -O){μ <sub>2</sub> -O <sub>2</sub> CN[SiMe <sub>2</sub> (CH <sub>2</sub> ) <sub>2</sub> ] <sub>2</sub> (μ <sub>2</sub> -N=C=O) <sub>2</sub> (4)	2.331(2) 2.164(3) 2.226(3) 2.429(3) 2.716(4) 2.165(3) 2.379(2) 2.225(3) 2.458(2)	na	1.274(58) 1.282(5) 1.272(5) 1.291(5) 1.273(6) 1.289(5) 1.301(6) 1.257(5)	na	1.349(5) 1.345(5) 1.355(5)	121.0(4) 121.1(4) 121.6(4)	121.3(4) 117.6(4) 118.2(4) 120.3(4) 116.9(4) 121.5(4)	IFOXEH 664586	[50]
[(Me <sub>2</sub> NCO <sub>2</sub> ) <sub>2</sub> Sn] <sub>2</sub> (5)	2.332(1) 2.235(2) 2.432(2) 2.115(2)	na	1.272(3) 1.280(3) 1.263(3) 1.295(3)	na	1.338(3) 1.336(3)	118.8(2) 121.8(2)	120.2(2) 121.0(2) 121.3(2) 116.9(2)	UYOBIU 806650	[52]
[HC{(Me)CN(2,6- <i>i</i> -Pr <sub>2</sub> C <sub>6</sub> H <sub>3</sub> ) <sub>2</sub> }] <sub>2</sub> SnOC(O)Ni-Pr <sub>2</sub> (6)	2.1346(16)	na	1.304(3)	1.238(3)	1.366(3)	121.7(2)	116.6(2) 121.7(2)	MIYHIN 791226	[53]

**Table 2.** Selection of spectroscopic data (NMR and IR) assigned to carbamates of tin complexes.

Compounds	<sup>119</sup> Sn{ <sup>1</sup> H} NMR (δ, ppm)	<sup>13</sup> C{ <sup>1</sup> H} NMR -NC(O)O- (δ, ppm)	IR ν(C=O) (cm <sup>-1</sup> )	Ref.
Sn(O <sub>2</sub> CNi-Pr <sub>2</sub> ) <sub>4</sub> (2)	−920.8 <sup>a</sup>	164.4 <sup>a</sup>	na	[45]
Sn(O <sub>2</sub> CNEt <sub>2</sub> ) <sub>4</sub> (3)	−930.0 <sup>b</sup>	166.2 <sup>b</sup>	1612	[46]
Sn <sub>4</sub> (μ <sub>4</sub> -O){μ <sub>2</sub> -O <sub>2</sub> CN[SiMe <sub>2</sub> (CH <sub>2</sub> ) <sub>2</sub> ] <sub>2</sub> (μ <sub>2</sub> -N=C=O) <sub>2</sub> (4)	−316.0 <sup>b</sup>	167.9 <sup>b</sup>	na	[50]
[(Me <sub>2</sub> NCO <sub>2</sub> ) <sub>2</sub> Sn] <sub>2</sub> (5)	−613.0 <sup>a</sup>	164.5 <sup>a</sup>	1651	[52]
[HC{(Me)CN(2,6- <i>i</i> -Pr <sub>2</sub> C <sub>6</sub> H <sub>3</sub> ) <sub>2</sub> }] <sub>2</sub> SnOC(O)Ni-Pr <sub>2</sub> (6)	−394.0 <sup>b</sup>	161.75 <sup>b</sup>	1595, 1575, 1552, and 1524	[53]
[HC{(Me)CN(2,6- <i>i</i> -Pr <sub>2</sub> C <sub>6</sub> H <sub>3</sub> ) <sub>2</sub> }] <sub>2</sub> SnOC(O)NH(2,6- <i>i</i> -Pr <sub>2</sub> C <sub>6</sub> H <sub>3</sub> ) (7)	−398.0 <sup>b</sup>	161.59 <sup>b</sup>	1624, 1554, 1526, and 1517	[53]

<sup>a</sup> Measured in chloroform-*d*; <sup>b</sup> measured in benzene-*d*<sub>6</sub>.

### 3. Formate Tin Complexes

#### 3.1. Early Works

To our knowledge, pioneering work on formate tin complexes dates back to 1927. Elöd and Kolbach described a general method to prepare a series of Sn(II) compounds of formula M<sub>2</sub>Sn(O<sub>2</sub>CH)<sub>4</sub>·5H<sub>2</sub>O (M = Na, K, and NH<sub>4</sub>) by dissolving tin(II) chloride into solutions of alkali metal or ammonium formate, in formic acid (35% *w/w*) [54]. In 1964, Donaldson and Knifton revisited the synthetic protocol by reporting the preparation and analysis of alkali metal (K, Rb, and Cs) and ammonium derivatives of the triformatostannate(II) anion [Sn(O<sub>2</sub>CH)<sub>3</sub>]<sup>−</sup> [55]. In 1969, Jelen and Lindqvist solved the crystal structure of potassium triformatostannate(II), KSn(HCO<sub>2</sub>)<sub>3</sub> in which the tin atom is coordinated pyramidally by three oxygen atoms of three formate groups (CSD refcode: KTFORM, 1200243) [56]. Thereafter in 1974, Harrison and Thornton published an X-ray diffraction study devoted to the structure determination of Sn(O<sub>2</sub>CH)<sub>2</sub> arranged in infinite two-dimensional sheets in which tin(II) atoms are bridged by formate groups (CSD refcode: SNFORM, 1260779) [57].

Solid-state structures of tin(IV) formate complexes were established from the 1980s. In 1987, Molloy et al. reported the crystal structure of triphenyltin formate prepared from a mixture of triphenyltin hydroxide and formic acid in refluxing toluene [58]. [Ph<sub>3</sub>Sn(O<sub>2</sub>CH)]<sub>*n*</sub> is organized in a polymeric chain propagating along *c* axis and compared by the au-

thors to a flattened helix. Triphenyltin moieties are bridged by bidentate formate ligands (CSD refcode: FAJZIZ, 1151980; Figure 6). In 1990, Mistry et al. resolved the structure of bis(formato)dimethyltin(IV),  $[\text{Me}_2\text{Sn}(\text{O}_2\text{CH})_2]_n$ , which was described as a sheet polymer with linear  $\text{Me}_2\text{Sn}$  moieties nearly symmetrically bridged by formate anions. Sn atoms exhibit an octahedral geometry (CCDC ref.: SIFLEY, 1258788; Figure 7) [59]. More recently, Power et al. published the synthesis and characterization of several organotin(IV) formates prepared from hydrides and hydroxides of organotins in the presence of formic acid [60]. X-ray crystallographic structures investigations were conducted on five compounds.  $[n\text{-Bu}_2\text{Sn}(\text{O}_2\text{CH})_2]_n$  (CCDC ref.: EKONEY, 783726; Figure 8),  $[(\text{PhCH}_2)_3\text{Sn}(\text{O}_2\text{CH})]_n$  (CCDC ref.: EKONAU, 783725), and  $[\text{Cy}_3\text{Sn}(\text{O}_2\text{CH})]_n$  (Cy = cyclohexyl) (crude structure owing to the low quality of crystals) exhibit polymeric structures, while  $\text{Mes}_3\text{SnOC}(\text{O})\text{H}$  (Mes = 2,4,6-trimethylphenyl) (CCDC ref.: EKONOI, 783728) and  $\text{Dmp}_3\text{SnOC}(\text{O})\text{H}$  (dmp = 2,6-dimethylphenyl) (CCDC ref.: EKONIC, 783727; Figure 9) are monomeric tin formates. In 2010, McMurtrie and Arnold reported the crystal structure of *meso*-tetraphenylporphyrinatotin(IV) diformate, prepared from  $\text{Sn}(\text{TPP})(\text{OH})_2$  (TPP = dianion of 5,10,15,20-tetraphenylporphyrin) and formic acid, and in which the central tin atom exhibits an octahedral geometry with two axially O-coordinated formate ligands (Figure 10) [61].

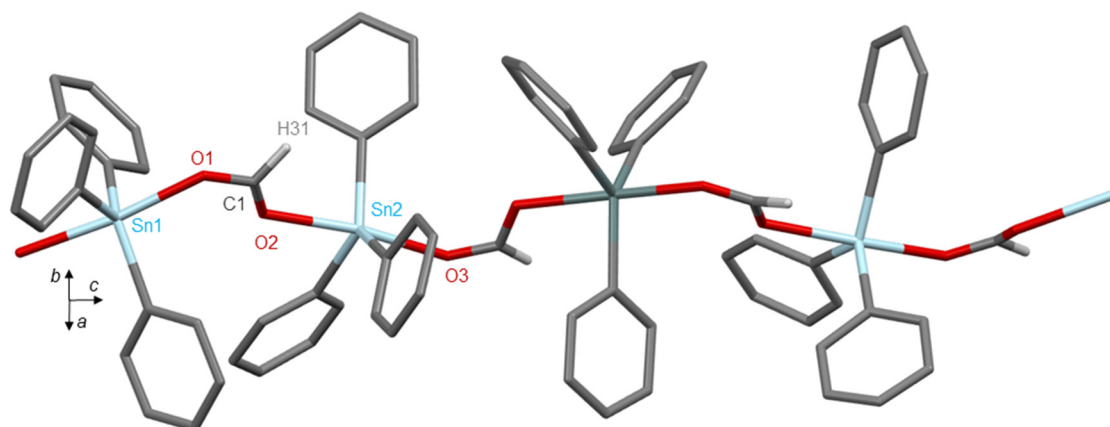


**Figure 6.** Molecular structure of  $[\text{Ph}_3\text{Sn}(\text{O}_2\text{CH})]_n$  (CSD refcode: FAJZIZ, 1151980), adapted from [58] (MERCURY view). Hydrogen atoms are omitted for clarity except that of the formate group (Sn light blue, O red, C grey, H white).

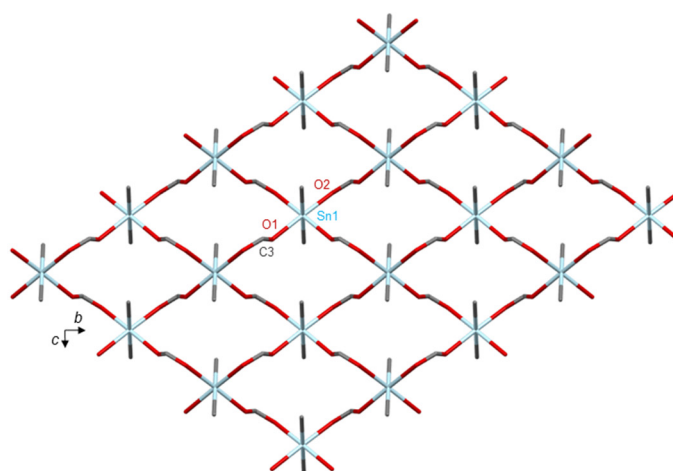


**Figure 7.** Infinite sheets based-structure of  $[\text{Me}_2\text{Sn}(\text{O}_2\text{CH})_2]_n$  (CCDC ref.: SIFLEY, 1258788), adapted from [59] (MERCURY view). Hydrogen atoms are omitted for clarity (Sn light blue, O red, C grey).

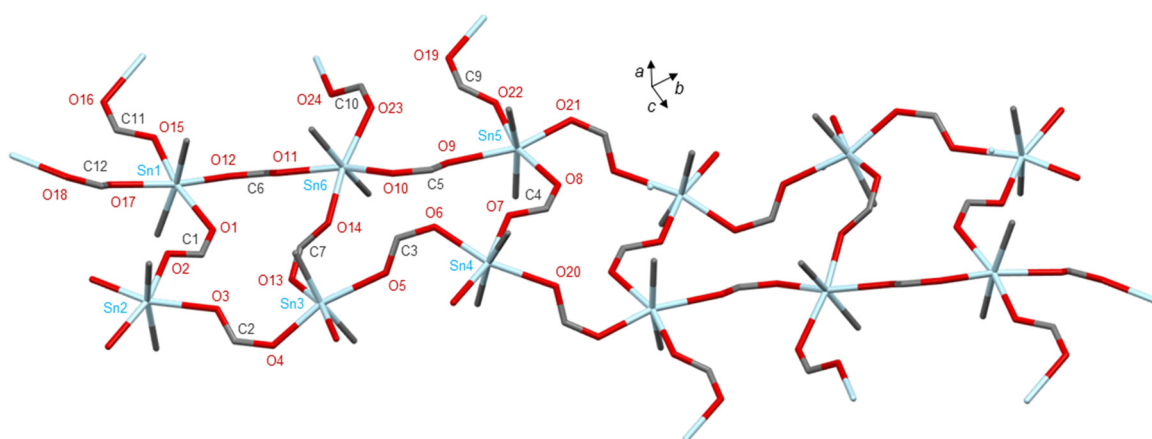


**Figure 8.** Polymeric structure of  $[n\text{-Bu}_2\text{Sn}(\text{O}_2\text{CH})_2]_n$  (CCDC ref.: EKONEY, 783726), adapted from [60] (MERCURY view). Hydrogen atoms are omitted for clarity and for each *n*-butyl chain; only the  $\alpha$ -carbon atoms bonded to tin are shown (Sn light blue, O red, C grey).

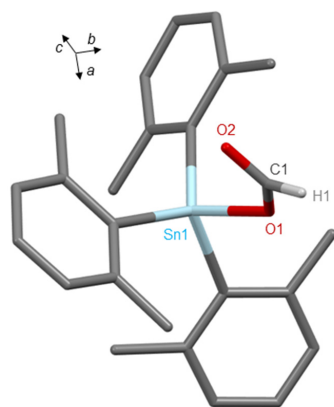


**Figure 9.** Molecular structure of  $\text{Dmp}_3\text{SnOC}(\text{O})\text{H}$  (dmp = 2,6-dimethylphenyl) (CCDC ref.: EKONIC, 783727), adapted from [60] (MERCURY view). Hydrogen atoms are omitted for clarity except that of the formate group (Sn light blue, O red, C grey, H white).

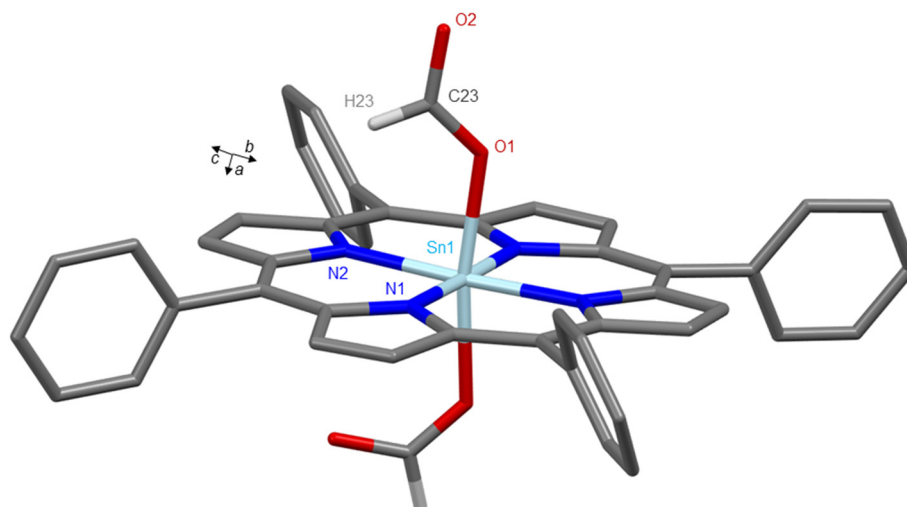
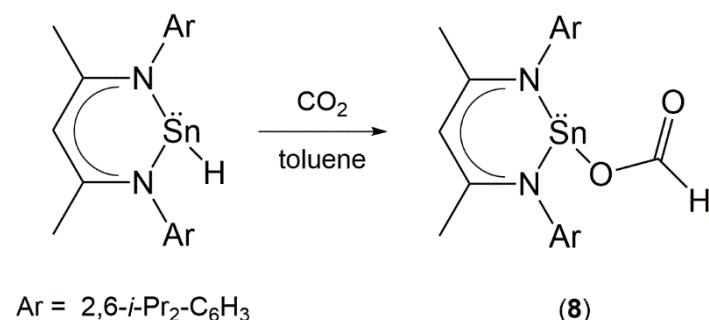


**Figure 10.** Molecular structure of  $\text{Sn}(\text{TPP})[(\text{OC}(\text{O})\text{H})_2]$  (TPP = dianion of 5,10,15,20-tetraphenylporphyrin) (CCDC ref.: EPAZAX, 711428), adapted from [61] (MERCURY view). Hydrogen atoms are omitted for clarity except that of the formate group (Sn light blue, O red, N dark blue, C grey, H white).

### 3.2. X-Ray Crystal Structures of Formato Tin Complexes Resulting from Reactivity with CO<sub>2</sub>

While the formation of the above compounds required the use of formic acid in their preparation, there are also a few examples of formato tin complexes directly isolated under carbon dioxide atmosphere, resulting from the insertion of CO<sub>2</sub> into the Sn–H bond. In our opinion, six complexes, published mainly during the last decade and characterized by X-ray diffraction, correspond to this category of compounds (Table 3). In 2009, Roesky et al. reported the structural and spectroscopic characterization of several complexes resulting from hydrostannylation reactions of carbon dioxide, ketones, aldehydes, alkynes and carbodiimides with the tin(II) hydride precursor, [HC{(Me)CN(2,6-*i*-Pr<sub>2</sub>C<sub>6</sub>H<sub>3</sub>)<sub>2</sub>}]<sub>2</sub>SnH [62]. In the case of the reaction involving CO<sub>2</sub>, bubbling at room temperature very quickly causes a change in color (from yellow to colorless) of the reaction mixture (toluene solution). The treatment with *n*-hexane then leads to the formation of a microcrystalline powder (at –32 °C) characterized as being the stannylene formate complex, [HC{(Me)CN(2,6-*i*-Pr<sub>2</sub>C<sub>6</sub>H<sub>3</sub>)<sub>2</sub>}]<sub>2</sub>SnOC(O)H (**8**) (Scheme 16). The presence of the formate ligand evidenced by infrared was confirmed by single-crystal X-ray diffraction. The molecular structure shows moreover a distorted *pseudo*-tetrahedral environment for the tin atom, completed by one electron lone pair (Figure 11).



**Scheme 16.** Reaction scheme leading to Compound **8**, data from [62].

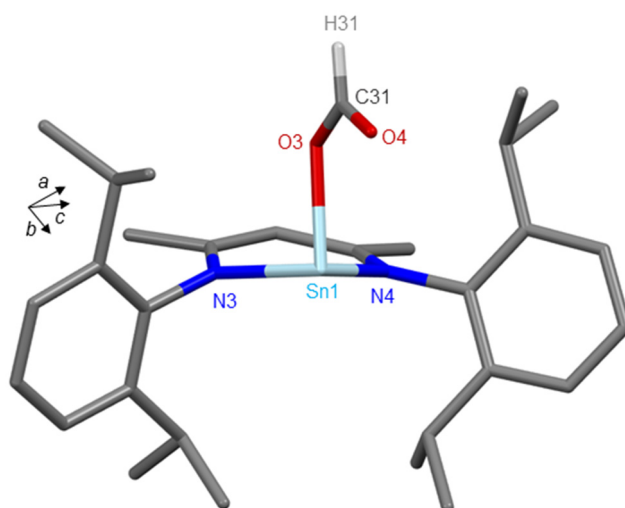
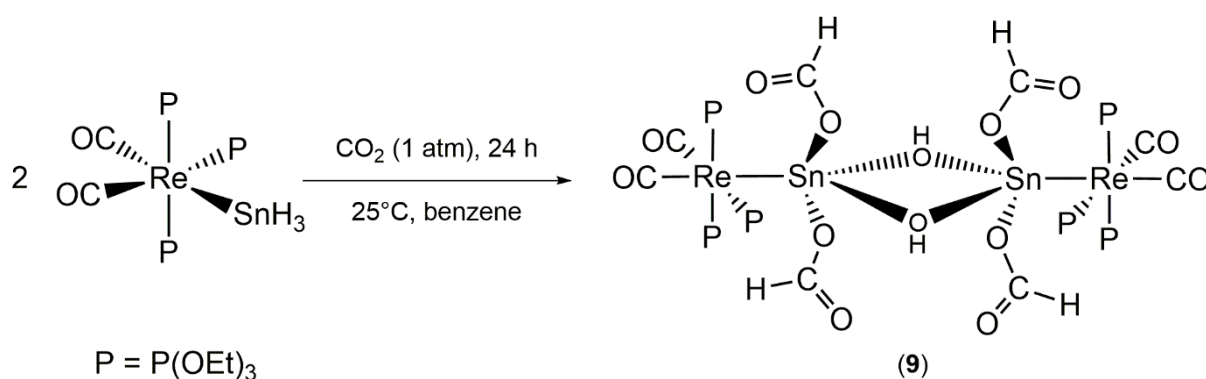


**Figure 11.** Molecular structure of **8**, adapted from [62] (MERCURY view). Hydrogen atoms are omitted for clarity except that of the formate group (Sn light blue, O red, N dark blue, C grey, H white).

During the period 2007–2010, the Albertin's group isolated several formato tin complexes by studying the reactivity of transition-metal stannyl complexes with carbon dioxide. Three of these complexes were characterized by single-crystal X-ray diffraction studies. Firstly, the reaction of Re(SnH<sub>3</sub>)(CO)<sub>2</sub>[P(OEt)<sub>3</sub>]<sub>3</sub>, in solution in benzene and at room temperature, with CO<sub>2</sub> (under atmospheric pressure) and during 24 h led to the binuclear OH-bridging bis(formate) complex [Re{Sn[OC(O)H]<sub>2</sub>(μ-OH)}(CO)<sub>2</sub>[P(OEt)<sub>3</sub>]<sub>2</sub> (**9**)

(Scheme 17) [63]. The authors described the core of **9** as a dimeric complex in which two octahedrally coordinated rhenium units are joined by a bridging tetraformatebis( $\mu$ -hydroxo)ditin moiety. Tin atoms exhibit a highly distorted square pyramidal coordination geometry, bearing two  $\eta^1$ -formate ligands per metal atom. The central  $\text{Sn}_2\text{O}_2$  distannoxane ring is planar (Figure 12). Infrared and  $^{13}\text{C}\{^1\text{H}\}$  NMR spectra attest also the presence of formates by showing two bands at  $1674\text{--}1594\text{ cm}^{-1}$  ( $\nu_{\text{OCO}}$ , asym) and one resonance at  $\delta$  166 ppm [ $\text{OC}(\text{O})\text{H}$ ], respectively (Table 4).



**Scheme 17.** Reaction scheme leading to compound **9**, data from [63].

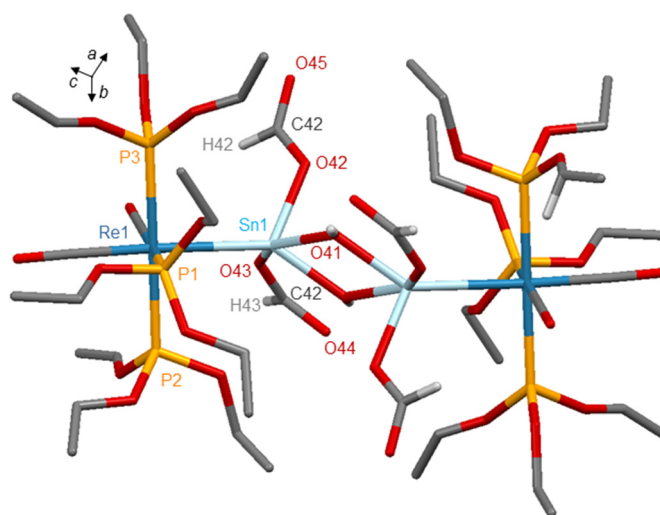
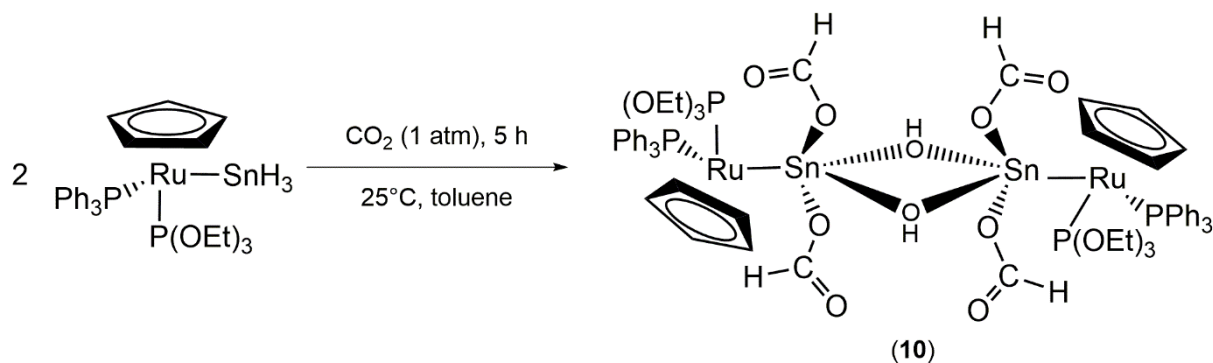


**Figure 12.** Molecular structure of **9**, adapted from [63] (MERCURY view). Hydrogen atoms are omitted for clarity except those of hydroxyl and formate groups (Re blue, Sn light blue, O red, P orange, C grey, H white).

In 2008, the same group reported a similar structure by standing the ruthenium-cyclopentadienyl-trihydridostannyl complex,  $\text{Ru}(\text{SnH}_3)(\text{Cp})[\text{P}(\text{OEt})_3](\text{PPh}_3)$ , under a  $\text{CO}_2$  atmosphere for 5 h (Scheme 18) [64]. The resulting formate species was characterized as  $[\text{Ru}[\text{Sn}\{\text{OC}(\text{O})\text{H}\}_2(\mu\text{-OH})](\text{Cp})\{\text{P}(\text{OEt})_3\}(\text{PPh}_3)_2]$  (**10**), exhibiting a structure based on two  $\mu\text{-OH}$  groups bridging the tin atoms (Figure 13).

In 2010, Albertin et al. studied the reactivity of hydride-trihydridestannyl complexes  $\text{MH}(\text{SnH}_3)_4$  [ $\text{M} = \text{Fe, Os}$ ;  $\text{P} = \text{P}(\text{OEt})_3, \text{PPh}(\text{OEt})_2$ ] toward carbon dioxide leading to solids characterized as hydroxobis(formate)stannyl derivatives,  $\text{MH}[\text{Sn}(\text{OH})\{\text{OC}(\text{O})\text{H}\}_2]\text{P}_4$  [65]. Reactions took place at room temperature, in solution in toluene and under atmospheric pressure of  $\text{CO}_2$  (Scheme 19). Starting from  $\text{OsH}(\text{SnH}_3)(\text{PPh}(\text{OEt})_2)_4$ , the compound  $\text{OsH}[\text{Sn}(\text{OH})\{\text{OC}(\text{O})\text{H}\}_2][\text{PPh}(\text{OEt})_2]_4$  (**11**) was obtained and its molecular structure was established by single-crystal X-ray diffraction showing the insertion of two  $\text{CO}_2$  molecules into two  $\text{Sn}\text{--}\text{H}$  bonds (Scheme 19). The  $\text{Os}\text{--}\text{H}$  bond remains intact. The hydride ligand is

unequivocally demonstrated by  $^1\text{H}$  NMR spectroscopy showing a multiplet at  $\delta -11$  ppm. The osmium atom is hexacoordinated according to a distorted octahedral geometry bearing four phosphonite ligands, one hydride ligand, and one hydroxobis(formate) stannyl ligand. The hydride and stannyl ligand are in *cis* positions. Regarding the coordination of the tin atom, Sn is tetracoordinate displaying a tetrahedral geometry (Figure 14).



**Scheme 18.** Reaction scheme leading to Compound 10, data from [64].

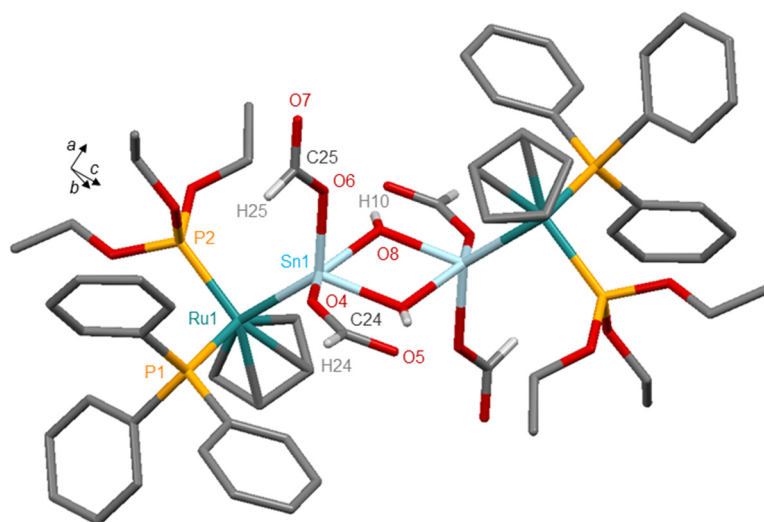
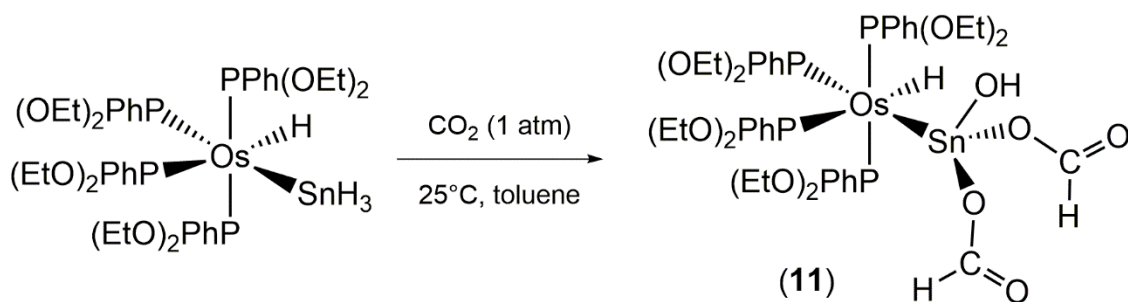


**Figure 13.** Molecular structure of 10, adapted from [64] (MERCURY view). Hydrogen atoms are omitted for clarity except those of hydroxyl and formate groups (Ru blue green, Sn light blue, O red, P orange, C grey, H white).



**Scheme 19.** Reaction scheme leading to Compound 11, data from [65].

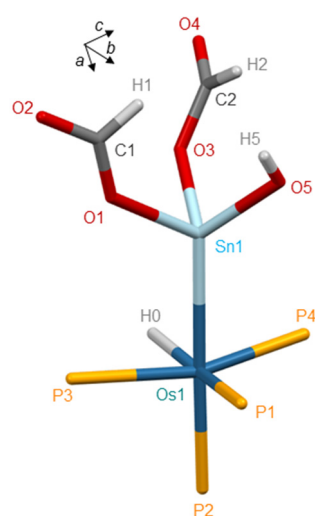


**Figure 14.** Molecular structure of **11**, adapted from [65] (MERCURY view). Ph and OEt substituents are omitted for clarity (Os blue, Sn light blue, O red, P orange, C grey, H white).

In 2016, Strohmann et al. published the crystal structure of diaquadi- $\mu$ -hydroxido-tris[trimethyltin(IV)] diformatotrimethylstannate(IV),  $[(\text{Me}_3\text{Sn})_3(\mu\text{-OH})_2(\text{H}_2\text{O})_2][\text{Me}_3\text{Sn}\{\text{OC}(\text{O})\text{H}\}_2]$  (**12**), obtained as byproduct from trapping reactions with trimethyltin chloride and formed from atmospheric  $\text{CO}_2$  [66]. The structure of **12** consists of a short trimethyltin hydroxide chain (tristannoxane), positively charged, and a bisformatostannate, negatively charged (Figure 15). From a supramolecular point of view, formate ligands bridge four cationic tristannoxanes via hydrogen-bonding interactions leading to a two-dimensional network.

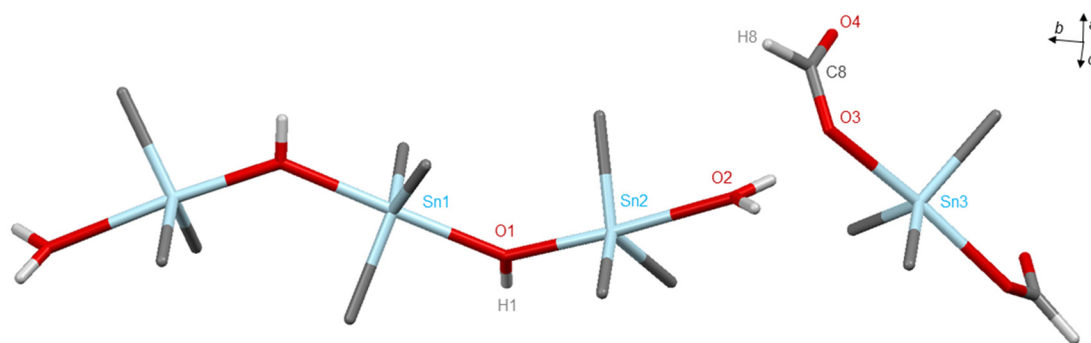
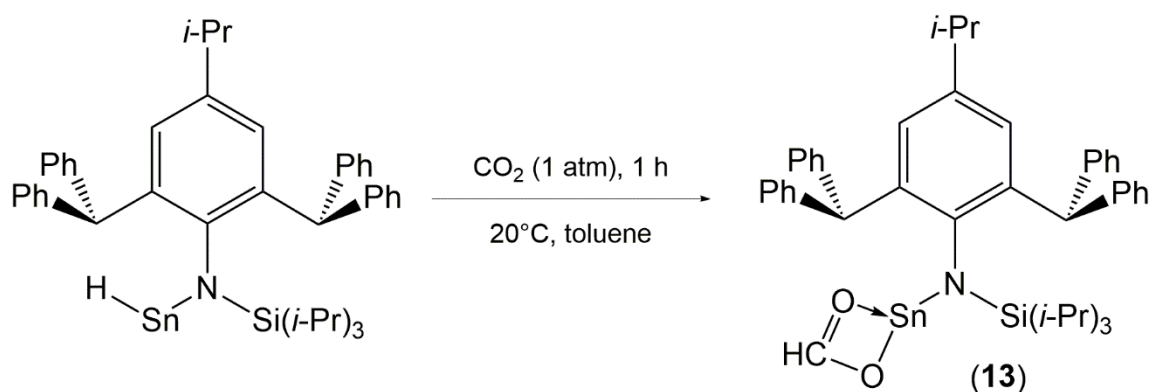


**Figure 15.** Molecular structure of **12**, adapted from [66] (MERCURY view). Hydrogen atoms of methyl groups are omitted for clarity (Sn light blue, O red, C grey, H white).

Lately, in 2017, Jones et al. reported the efficient and highly selective use of the two-coordinate amido-tin(II) hydride complex,  $\text{LSnH}$  ( $\text{L} = -\text{N}(\text{C}_6\text{H}_2\text{-}i\text{-Pr}\{\text{C}(\text{H})\text{Ph}_2\}_2\text{-}4,2,6)(\text{Si-}i\text{-Pr}_3)$ ), acting as catalytic species for the reductive hydroboration of  $\text{CO}_2$  into methanol equivalents,  $\text{MeOBR}_2$  (2-methoxy-4,4,5,5-tetramethyl-1,3,2-dioxaborolane and catecholoboronyl methoxide), using boranes,  $\text{HBR}_2$ , as hydrogen sources [67]. The tin formate complex,  $\text{LSn}(\kappa^2\text{-O, O'}\text{-O}_2\text{CH})$  (**13**), was thus isolated during catalytic studies and also by exclusively reacting  $\text{LSnH}$  with  $\text{CO}_2$  (Scheme 20) or alternatively from  $\text{LSnBr}$  with potassium formate,  $\text{KOC}(\text{O})\text{H}$ . Compound **13** was crystallographically characterized and consists of a monomeric complex in which the tin atom is unusually chelated by a formate ligand (Figure 16).



**Scheme 20.** Reaction scheme leading to Compound 13, data from [67].

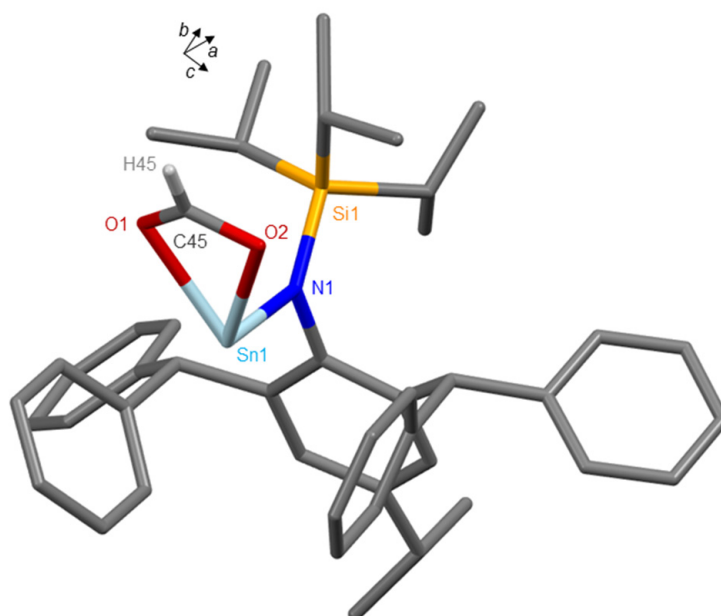


**Figure 16.** Molecular structure of 13, adapted from [67] (MERCURY view). Hydrogen atoms are omitted for clarity except that of the formate group (Sn light blue, O red, N dark blue, Si orange, C grey, H white).

**Table 3.** Comparison of selected structural parameters found in formates of organotin complexes.

Compounds	Sn–O(C) (Å)	C–O(Sn) (Å)	C–O (Å)	Sn–O–C (deg)	O–C–O (deg)	CSD Entry Deposition Number	Ref.
[HC(Me)CN(2,6- <i>i</i> -Pr <sub>2</sub> C <sub>6</sub> H <sub>3</sub> ) <sub>2</sub> ]SnOC(O)H (8)	2.1353(15)	1.299(2)	1.209(3)	116.40(13)	126.78(18)	COPLOJ 709476	[62]
[Re{Sn[OC(O)H] <sub>2</sub> (μ-OH)}(CO) <sub>2</sub> {P(OEt) <sub>3</sub> } <sub>2</sub> ] (9)	2.040(5) 2.071(7)	1.29(1) 1.26(1)	1.19(2) 1.21(1)	123.1(6) 132.2(6)	126(1) 128.8(9)	CIHYUO 655465	[63]
[Ru{Sn[OC(O)H] <sub>2</sub> (μ-OH)}(Cp){P(OEt) <sub>3</sub> }(PPh <sub>3</sub> ) <sub>2</sub> ] (10)	2.210(2) 2.069(2)	1.262(4) 1.274(5)	1.216(5) 1.205(6)	128.7(2) 133.5(2)	127.9(3) 125.7(4)	KOMBUK 708897	[64]
OsH[Sn(OH){OC(O)H] <sub>2</sub> ][PPh(OEt) <sub>2</sub> ] <sub>4</sub> (11)	2.061(5) 2.089(5)	1.16(1) 1.25(1)	1.11(1) 1.21(1)	132.8(7) 124.9(7)	131(1) 124(1)	ALAGUO 813529	[65]
[(Me <sub>3</sub> Sn) <sub>3</sub> (μ-OH) <sub>2</sub> (H <sub>2</sub> O) <sub>2</sub> ][Me <sub>3</sub> Sn{OC(O)H} <sub>2</sub> ] (12)	2.2991(17) 2.2990(17)	1.269(3)	1.224(3)	125.94(17)	128.1(3)	EWIGIC 1505528	[66]
N(C <sub>6</sub> H <sub>2</sub> - <i>i</i> -Pr[C(H)Ph] <sub>2</sub> -4,2,6)(Si- <i>i</i> -Pr <sub>3</sub> )Sn(κ <sup>2</sup> -O,O'-O <sub>2</sub> CH) (13)	2.353(2) 2.333(2)	1.109(4) 1.310(4)	na	91.4(2) 87.5(2)	125.6(4)	ACEQUX 1518144	[67]

**Table 4.** Selection of spectroscopic data (NMR and IR) assigned to formates of tin complexes.

Compounds	$^{119}\text{Sn}\{^1\text{H}\}$ NMR ( $\delta$ , ppm)	$^{13}\text{C}\{^1\text{H}\}$ NMR –OC(H)O ( $\delta$ , ppm)	$^1\text{H}$ NMR –OC(H)O ( $\delta$ , ppm)	IR ( $\text{cm}^{-1}$ )	Ref.
[HC{(Me)CN(2,6- <i>i</i> -Pr <sub>2</sub> C <sub>6</sub> H <sub>3</sub> ) <sub>2</sub> } <sub>2</sub> SnOC(O)H (8)	−360 <sup>a</sup>	166.92 <sup>a</sup>	8.97 $^3J(^{119}\text{Sn},\text{H}) = 52 \text{ Hz}$	1641 ( $\nu_{\text{C=O}}$ ) 2700 ( $\nu_{\text{C-H}}$ )	[62]
[Re{Sn[OC(O)H] <sub>2</sub> ( $\mu$ -OH)}(CO) <sub>2</sub> {P(OEt) <sub>3</sub> } <sub>3</sub> ] (9)	−487.7 <sup>b</sup>	166.4 <sup>b</sup>	9.21 <sup>bc</sup>	1665, 1594 ( $\nu_{\text{CHO}}$ )	[63]
[Ru{Sn[OC(O)H] <sub>2</sub> ( $\mu$ -OH)}(Cp){P(OEt) <sub>3</sub> }(PPh <sub>3</sub> ) <sub>2</sub> ] (10)	−263.5 <sup>cd</sup>	166.1 <sup>d</sup>	8.36 <sup>d</sup>	1660, 1627 ( $\nu_{\text{CHO}}$ )	[64]
OsH[Sn(OH){OC(O)H] <sub>2</sub> ][PPh(OEt) <sub>2</sub> ] <sub>4</sub> (11)	−451.0 <sup>b</sup>	165.5 <sup>e</sup>	8.93 <sup>b</sup>	1673, 1634 ( $\nu_{\text{CHO}}$ )	[65]
N(C <sub>6</sub> H <sub>2</sub> - <i>i</i> -Pr(C(H)Ph) <sub>2</sub> -4,2,6)(Si- <i>i</i> -Pr <sub>3</sub> )Sn( $\kappa^2$ -O,O'-O <sub>2</sub> CH) (13)	−134.0 <sup>a</sup>	173.80 <sup>a</sup>	8.71 <sup>a</sup>	1549 ( $\nu_{\text{CHO}}$ )	[67]

<sup>a</sup> Measured in benzene-d<sub>6</sub>; <sup>b</sup> measured in toluene-d<sub>8</sub>; <sup>c</sup> measured at −70 °C; <sup>d</sup> measured in acetone-d<sub>6</sub>; <sup>e</sup> determined for OsH[Sn(OH){OC(O)H]<sub>2</sub>][P(OEt)<sub>3</sub>]<sub>4</sub>.

## 4. Phosphinoformato Tin Complexes

### 4.1. Foreword

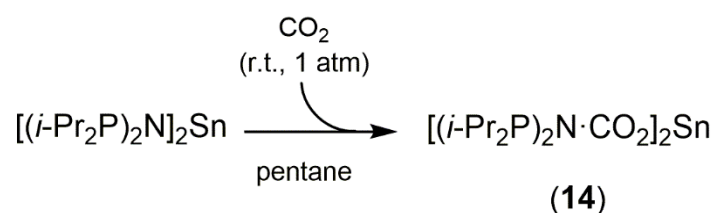
This type of compound, rarely described so far, results from the insertion of CO<sub>2</sub> into the Sn–P bond then leads to the formation of the Sn–OC(O)P moiety which can be qualified as a phosphinoformato derivative, by analogy with phosphino formic acid (H<sub>2</sub>PCOOH) according to the recent work published by Kaiser et al. [68]. To the best of our knowledge, only two examples of this type of complex have been described so far (Table 5), and their characterization is quite recent (last decade).

**Table 5.** Selection of structural parameters found in complexes 14 and 15.

Compounds	Sn–O(C) (Å)	P–C(O <sub>2</sub> ) (Å)	C–O(Sn) (Å)	C–O <sub>exo</sub> (Å)	Sn–O–C (deg)	O–C–O (deg)	O–C–P (deg)	CSD Entry Deposition Number	Ref.
[( <i>i</i> -Pr <sub>2</sub> P) <sub>2</sub> N·CO <sub>2</sub> ] <sub>2</sub> Sn (14)	2.344(4) 2.344(5)	1.875(7) 1.867(6)	1.272(8) 1.273(8)	1.210(8) 1.231(7)	128.2(5) 132.2(4)	126.8(6) 129.5(6)	114.5(5) 116.0(5) 117.8(5) 115.4(5)	RANBUF 831553	[69]
(F <sub>5</sub> C <sub>2</sub> ) <sub>3</sub> SnCH <sub>2</sub> P( <i>t</i> -Bu) <sub>2</sub> ·CO <sub>2</sub> (15)	2.233(2)	1.891(6)	1.268(4)	1.216(4)	122.9(2)	128.1(3)	114.9(2) 117.0(3)	FONREI 1892689	[70]

### 4.2. X-Ray Crystal Structures

The first example of the phosphinoformato tin complex, characterized by X-ray diffraction as [(*i*-Pr<sub>2</sub>P)<sub>2</sub>N·CO<sub>2</sub>]<sub>2</sub>Sn (14), was resolved in 2011 by Kemp et al. [69]. Complex 14 was isolated as a white precipitate by bubbling CO<sub>2</sub> at room temperature (for 10 min) through a pentane solution of [(*i*-Pr<sub>2</sub>P)<sub>2</sub>N]<sub>2</sub>Sn, which caused a color change of the solution from orange to yellow (Scheme 21). Structural analysis of single-crystals confirmed the capture of two molecules of CO<sub>2</sub> by [(*i*-Pr<sub>2</sub>P)<sub>2</sub>N]<sub>2</sub>Sn forming a six-membered ring complex in which CO<sub>2</sub> is inserted into one Sn–P bond of each ligand (Figure 17). Moreover, the authors studied the stability of 14 in particular by thermogravimetric analysis and showed the easy release of CO<sub>2</sub> from 90 °C. They showed also the possibility of recovering the starting complex by simply heating a solid sample of 14 under argon. Compound 14 is stable for several months stored under CO<sub>2</sub> at room temperature or under argon at −25 °C. On the basis of these observations, the incorporation of CO<sub>2</sub> as an adduct is preferentially considered rather than as a real insertion.



**Scheme 21.** Reaction scheme leading to Compound **14**, data from [69].

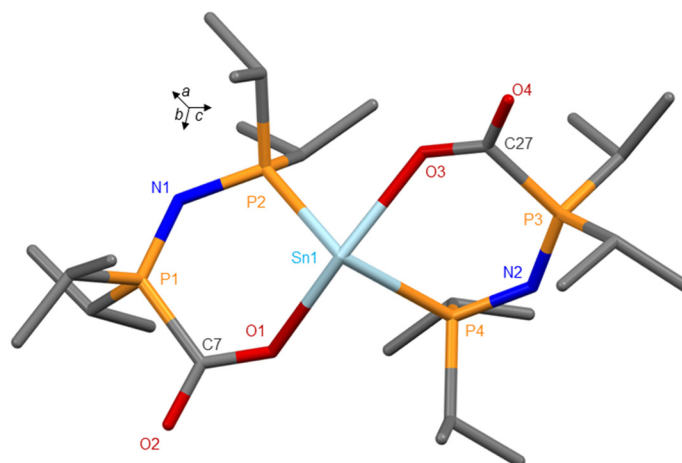
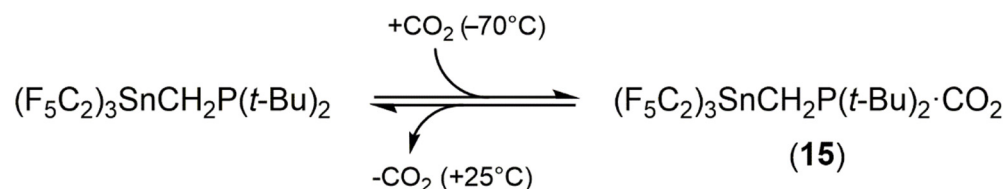


**Figure 17.** Molecular structure of **14**, adapted from [69] (MERCURY view). Hydrogen atoms are omitted for clarity (Sn light blue, O red, P orange, N dark blue, C grey).

More recently, in 2019, Mitzel et al. reported the reactivity of the *geminal* frustrated Lewis pair  $(\text{F}_5\text{C}_2)_3\text{SnCH}_2\text{P}(t\text{-Bu})_2$  with a variety of small molecules and, in particular, with  $\text{CO}_2$  [70]. The formation of the  $\text{CO}_2$  adduct of  $(\text{F}_5\text{C}_2)_3\text{SnCH}_2\text{P}(t\text{-Bu})_2$ , characterized as  $(\text{F}_5\text{C}_2)_3\text{SnCH}_2\text{P}(t\text{-Bu})_2\cdot\text{CO}_2$  (**15**), was first demonstrated by NMR at  $-70^\circ\text{C}$  in  $\text{THF-d}_8$  (Table 6). The authors mention the instability of the complex at room temperature causing the release of  $\text{CO}_2$  (Scheme 22). The  $\text{CO}_2$  molecule is bonded to tin and phosphorus atoms, thus leading to the formation of a five-membered ring with an exocyclic C–O bond. The  $\text{PCO}_2$  unit is planar (Figure 18). Other adducts resulting from the reactivity of  $(\text{F}_5\text{C}_2)_3\text{SnCH}_2\text{P}(t\text{-Bu})_2$ , in particular with  $\text{SO}_2$  and  $\text{CS}_2$ , were also isolated in the solid state and describe comparable solid-state structures.



**Scheme 22.** Reaction scheme leading to Compound **15**, data from [70].

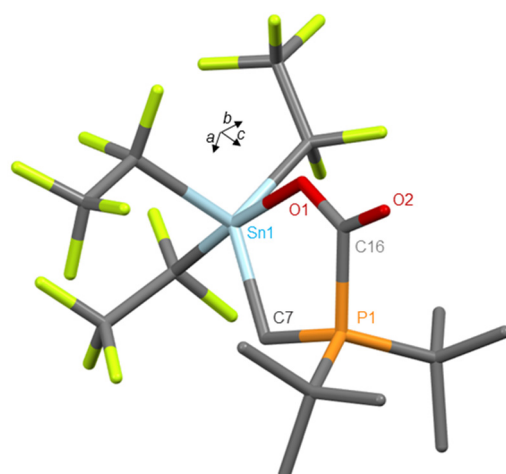


**Figure 18.** Molecular structure of **15**, adapted from [70] (MERCURY view). Hydrogen atoms are omitted for clarity (Sn light blue, O red, P orange, C grey, F green).

**Table 6.** Selection of spectroscopic data (NMR and IR) assigned to phosphinoformato of tin complexes.

Compounds	$^{119}\text{Sn}\{^1\text{H}\}$ NMR ( $\delta$ , ppm)	$^{13}\text{C}\{^1\text{H}\}$ NMR –OC(O)P ( $\delta$ , ppm)	$^{31}\text{P}\{^1\text{H}\}$ NMR –OC(O)P ( $\delta$ , ppm)	IR ( $\text{cm}^{-1}$ )	Ref.
$[(i\text{-Pr}_2\text{P})_2\text{N}\cdot\text{CO}_2]_2\text{Sn}$ ( <b>14</b> )	–184 <sup>a</sup> (t, $^1J_{\text{Sn-P}} = 2626$ Hz)	168.7 <sup>a</sup> (d, $^1J_{\text{C-P}} = 95$ Hz, $\text{PCO}_2$ )	26.4 <sup>a</sup> (s, broad)	1629 ( $\nu_{\text{C=O}}$ ) 1206	[69]
$(\text{F}_5\text{C}_2)_3\text{SnCH}_2\text{P}(\text{tBu})_2\cdot\text{CO}_2$ ( <b>15</b> )	–308.3 <sup>bc</sup> (hept, very broad, $^2J_{\text{Sn,F}} = 368$ Hz).	162.3 <sup>bd</sup> (d, $^1J_{\text{C-P}} = 80$ Hz, $\text{PCO}_2$ )	31.8 <sup>bd</sup> (s, $^2J_{\text{Sn,P}} = 56$ Hz)	na	[70]

<sup>a</sup> Measured in benzene- $d_6$ ; <sup>b</sup> measured in tetrahydrofuran- $d_8$ ; <sup>c</sup> determined at 208 K; <sup>d</sup> determined at 203 K.

## 5. Metalloxy-carboxylato Tin Complexes

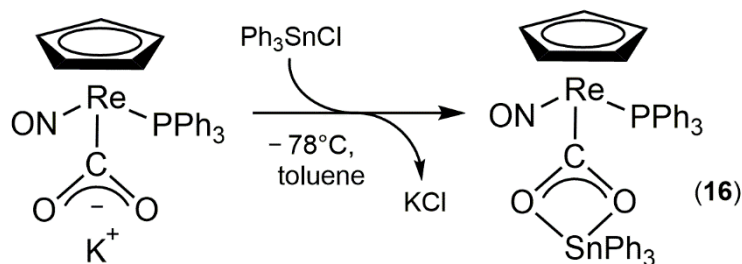
### 5.1. Foreword

The last part of this collection is devoted to bimetallic transition-metal/tin complexes with bridging carbon dioxide, of general formula  $\text{M}(\text{CO}_2)\text{Sn}$ , also named metalloxy-carboxylato tin complexes. Compared to the categories previously described, their synthesis does not involve the direct use of  $\text{CO}_2$  but is based on the reactivity between metalloxy-carboxylic acids and halogenated precursors of organotin. However, we have found it interesting and complementary to also include this class of compounds in this review. Metalloxy-carboxylato complexes and in particular tin derivatives began to be studied in the mid-1980s, often considered as suitable models of intermediates for the catalytic conversion of carbon dioxide [4]. Most of the structures shown below were resolved in the 1990s. The D. Gibson's group in Louisville (USA) was one of the most active in this field characterizing several of these compounds. Metalloxy-carboxylato-tin complexes have also been the subject of specific infrared considerations [71]. Indeed,  $\nu_{\text{OCO}}$  adsorption bands constitute well-suited probes for orienting and determining the coordination modes of the  $\text{CO}_2$  ligand.

### 5.2. X-Ray Crystal Structures

To the best of our knowledge, in 1987, Gladysz et al. reported the first X-ray characterization of a transition metal/tin bridging  $\text{CO}_2$  complex by isolating  $(\eta\text{-C}_5\text{H}_5)\text{Re}(\text{NO})(\text{PPh}_3)(\text{CO}_2\text{SnPh}_3)$  (**16**) [72]. Compound **16** was obtained in high yield (86%) by reacting  $(\eta\text{-C}_5\text{H}_5)\text{Re}(\text{NO})(\text{PPh}_3)(\text{CO}_2\text{K})$  with 1.1 equivalent of  $\text{Ph}_3\text{SnCl}$  at  $-78$  °C in THF (Scheme 23). Yellow crystal prisms of **16** grew from a mixture of  $\text{CH}_2\text{Cl}_2$ /hexane. Compound **16** is air- and water-stable, and could also be alternatively prepared from  $(\eta\text{-C}_5\text{H}_5)\text{Re}(\text{NO})(\text{PPh}_3)(\text{CO}_2\text{H})$  and  $(\text{Ph}_3\text{Sn})_2\text{O}$  at 25 °C in THF. Moreover, the decarboxylation of **16** occurs by heating at 180 °C for 10 min (from solid) or at 140 °C, for 20 h in solution in xylene. Using  $\text{Me}_3\text{SnCl}$ , the authors claim the formation of the analogue  $(\eta\text{-C}_5\text{H}_5)\text{Re}(\text{NO})(\text{PPh}_3)(\text{CO}_2\text{SnMe}_3)$  with a yield of 95%. The study was also extended to the synthesis of rhenium/germanium

and rhenium/lead bridging CO<sub>2</sub> complexes using Ph<sub>3</sub>GeBr and Ph<sub>3</sub>PbCl, as precursors, respectively. The crystallographic structure of **16** confirms the presence of two moieties based on rhenium and tin, respectively, linked by a CO<sub>2</sub> bridging ligand. The tin atom of **16** adopts a distorted trigonal bipyramid geometry in which the equatorial positions are occupied by the two oxygen atoms of the CO<sub>2</sub> ligand and supplemented by a phenyl group (Figure 19). The CO<sub>2</sub> ligand can be regarded as a carboxylato fragment, which is corroborated by infrared analysis, bidentally bound to the tin atom and defined as  $\mu(n^1\text{-C:}n^2\text{-O,O'})$  ligand.



Scheme 23. Reaction scheme leading to Compound **16**, data from [72].

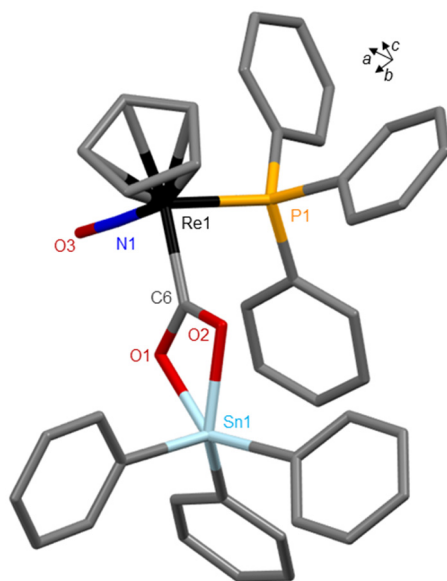
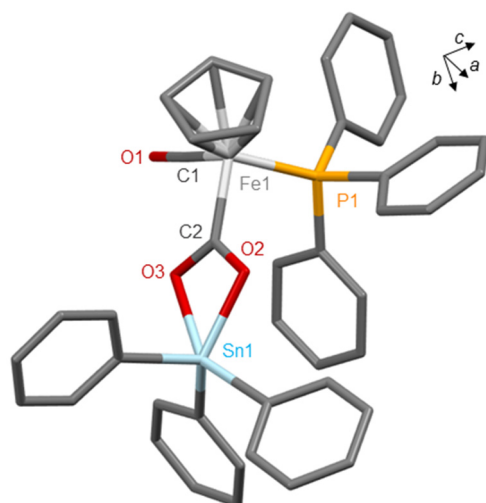


Figure 19. Molecular structure of **16**, adapted from [72] (MERCURY view). Hydrogen atoms are omitted for clarity (Sn light blue, O red, P orange, N dark blue, Re black, C grey).

In 1991, Gibson et al. published the solid state structure of  $(\eta\text{-C}_5\text{H}_5)\text{Fe}(\text{CO})(\text{PPh}_3)(\text{CO}_2\text{SnPh}_3)$  (**17**) prepared by mixing, under nitrogen and at low temperature, Ph<sub>3</sub>SnCl to a THF solution of CpFe(CO)(PPh<sub>3</sub>)COOK·3H<sub>2</sub>O [73]. The structure was found to be isomorphous to **16**, with the tin atom occupying a trigonal bipyramid arrangement (Figure 20). Compared to the Gladysz complex, the authors underline for **17** a greater difference between the lengths of the Sn–O bonds, corresponding to a value of 0.219 Å (Table 7). However, in the literature devoted to triaryltin organocarboxylate monomers this difference is generally much more marked in the range of 0.48 to 0.81 Å [74].



**Figure 20.** Molecular structure of **17**, adapted from [73] (MERCURY view). Hydrogen atoms are omitted for clarity (Sn light blue, O red, P orange, Fe white, C grey).

Two years later in 1993, the same group reported the solid state isolation of a new Fe/Sn CO<sub>2</sub>-bridged complex, which was characterized by single crystal X-ray diffraction analysis as the indenyl derivative ( $\eta^5$ -C<sub>9</sub>H<sub>7</sub>)Fe(CO)(PPh<sub>3</sub>)(CO<sub>2</sub>SnPh<sub>3</sub>) (**18**). Compound **18** was prepared under nitrogen, in THF solution and at 273 K, from ( $\eta^5$ -C<sub>9</sub>H<sub>7</sub>)Fe(CO)<sub>2</sub>(PPh<sub>3</sub>)<sup>+</sup>·I<sup>−</sup> and Ph<sub>3</sub>SnCl [75]. As shown by the structure displayed in Figure 21, the Sn atom geometry consists of a distorted trigonal bipyramid. However, the steric hindrance of the indenyl ligand and the resulting interactions with the phosphine ligand are suspected to cause notable structural differences compared to complexes **16** and **17**: (i) Sn–O bond lengths differ from 0.467(3) Å; (ii) the difference in the carboxyl C–O bond lengths also increases [0.100(4) Å]; (iii) the Fe–C–O bond angles exhibit higher distortions [10.2(3)°] (Table 7).

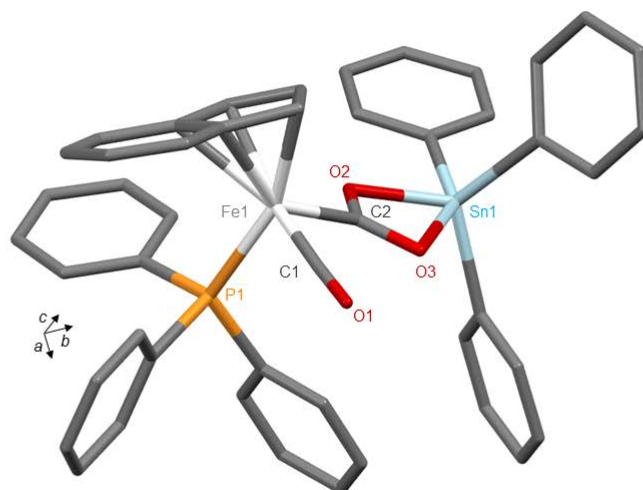


**Figure 21.** Molecular structure of **18**, adapted from [75] (MERCURY view). Hydrogen atoms are omitted for clarity (Sn light blue, O red, P orange, Fe white, C grey).

The Gibson's group continued to be very prolific in this field until the end of the 1990s, structurally characterizing several new iron and rhenium/tin CO<sub>2</sub> bridged complexes. In 1994, the reaction of Cp\*Re(CO)(NO)COOH with Ph<sub>3</sub>SnCl in the presence of Na<sub>2</sub>CO<sub>3</sub> afforded the formation of Cp\*Re(CO)(NO)(CO<sub>2</sub>SnPh<sub>3</sub>) (**19**) showing a  $\mu_2$ - $\eta^3$  coordination mode for the CO<sub>2</sub> ligand (Figure 22) [76]. As reflected by the lengths of the Sn–O and C–O bonds (Table 7), an asymmetric bonding mode of carboxylic oxygens to carbon and tin atoms was observed.

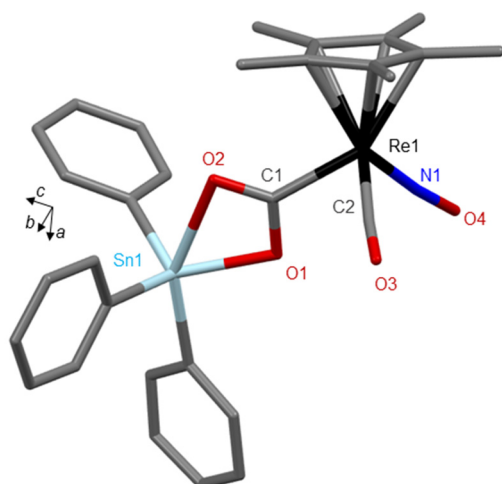


**Figure 22.** Molecular structure of **19**, adapted from [76] (MERCURY view). Hydrogen atoms are omitted for clarity (Sn light blue, O red, P orange, N blue, Re black, C grey).

In 1995, Gibson et al. resolved by X-ray diffraction, the structure of four new CO<sub>2</sub>-bridged transition metals/tin complexes [77]. CpFe(CO)(PPh<sub>3</sub>)(CO<sub>2</sub>SnMe<sub>3</sub>) (**20**) and CpFe(CO)(PPh<sub>3</sub>)(CO<sub>2</sub>Sn(*n*-Bu)<sub>3</sub>) (**21**) were synthesized by reaction in THF between CpFe(CO)(PPh<sub>3</sub>)CO<sub>2</sub><sup>−</sup>K<sup>+</sup> and ClSnMe<sub>3</sub> and ClSnPh<sub>3</sub>, respectively. In both cases, the bridging carboxyl ligand adopts a  $\mu_2\text{-}\eta^3$  coordination mode in which the carboxyl atom is bound to the iron atom and both oxygens are bound to the tin atom. Cp\*Fe(CO)<sub>2</sub>(CO<sub>2</sub>SnPh<sub>3</sub>) (**22**) was prepared from Cp\*Fe(CO)<sub>3</sub><sup>+</sup>BF<sub>4</sub><sup>−</sup> and Ph<sub>3</sub>SnCl in CH<sub>2</sub>Cl<sub>2</sub> at 0 °C in the presence of KOH. Compound **22** displays a similar structure to that of complexes **20** and **21** in which tin atoms are five-coordinated and adopt a distorted trigonal-bipyramidal geometry. The CO<sub>2</sub>-bridged rhenium-tin complex Cp\*Re(CO)(NO)(CO<sub>2</sub>SnMe<sub>3</sub>) (**23**) was isolated as crystalline solid from Cp\*Re(CO)(NO)COOH and ClSnMe<sub>3</sub> in the presence of KOH. The X-ray structure of **23** highlighted a  $\mu_2\text{-}\eta^2$  coordination mode of the bridging CO<sub>2</sub> ligand in which the carbonyl carbon and one oxygen atom are bonded to the rhenium atom and the tin atom, respectively. As a result, the tin atom adopts a distorted tetrahedral geometry (Figure 23).

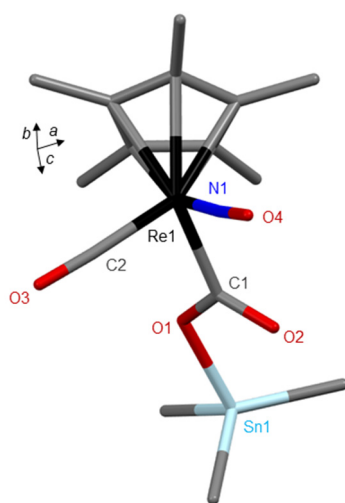
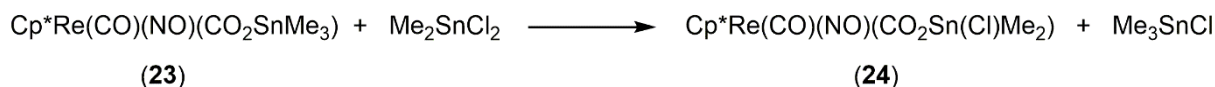


**Figure 23.** Molecular structure of **23**, adapted from [77] (MERCURY view). Hydrogen atoms and one molecule of CHCl<sub>3</sub> are omitted for clarity (Sn light blue, O red, N blue, Re black, C grey).

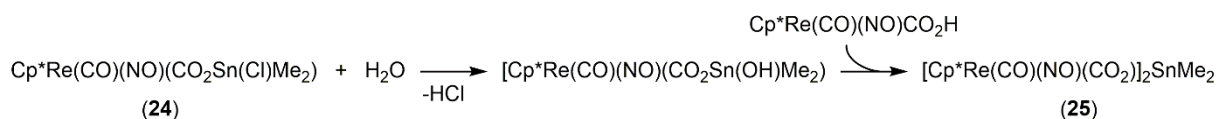
In 1997, two new specimen of CO<sub>2</sub>-bridged rhenium/tin complexes were characterized at the solid-state by the Gibson's group [78]. The transmetalation reaction involving

$\text{Cp}^*\text{Re}(\text{CO})(\text{NO})(\text{CO}_2\text{SnMe}_3)$  (**23**) and  $\text{Me}_2\text{SnCl}_2$  led to the formation in good yield of  $\text{Cp}^*\text{Re}(\text{CO})(\text{NO})(\text{CO}_2\text{Sn}(\text{Cl})\text{Me}_2)$  (**24**) jointly with  $\text{Me}_3\text{SnCl}$  (Scheme 24). The X-ray structure of complex **24** shows the presence of a  $\mu_2\text{-}\eta^3$   $\text{CO}_2$  ligand bridging the two moieties of rhenium and tin. The tin atom exhibits a five-coordinate geometry adopting an edge-capped tetrahedral arrangement rather than a distorted trigonal bipyramid.



**Scheme 24.** Reaction scheme leading to compound **24**, data from [78].

An equimolar mixture of  $\text{Cp}^*\text{Re}(\text{CO})(\text{NO})\text{COOH}$  and compound **24** leads, in the presence of water, to the formation of  $[\text{Cp}^*\text{Re}(\text{CO})(\text{NO})(\text{CO}_2)]_2\text{SnMe}_2$  (**25**) via the formation of an hydroxyl species, suggested by the authors as being  $\text{Cp}^*\text{Re}(\text{CO})(\text{NO})(\text{CO}_2\text{Sn}(\text{OH})\text{Me}_2)$  (Scheme 25). Complex **25** was also isolated by reacting  $\text{Cp}^*\text{Re}(\text{CO})(\text{NO})\text{COOH}$  with  $\text{Me}_2\text{SnCl}_2$  in the presence of  $\text{Na}_2\text{CO}_3$ . The structure of **25** was described as two  $\text{Cp}^*\text{Re}(\text{CO})(\text{NO})$  units linked to a  $\text{SnMe}_2$  moiety through two  $\mu_2\text{-}\eta^3$   $\text{CO}_2$  ligands. The central tin atom is hexacoordinated and displayed a skewed trapezoidal-bipyramidal geometry (Figure 24).



**Scheme 25.** Reaction scheme leading to compound **25**, data from [78].

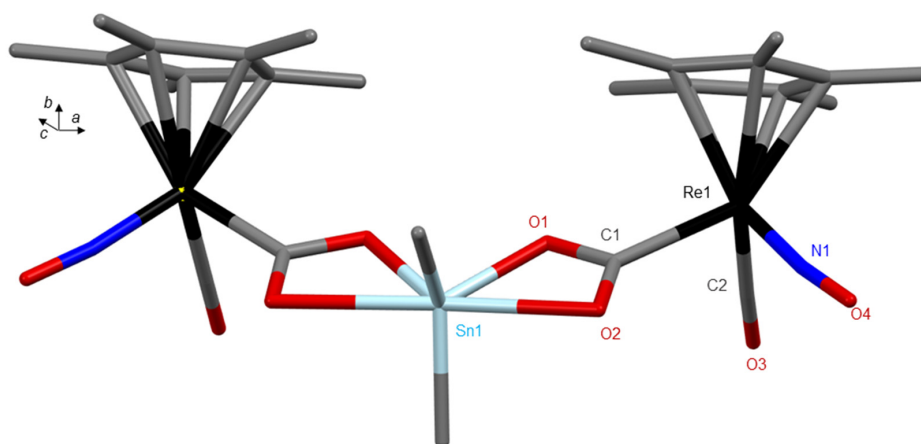
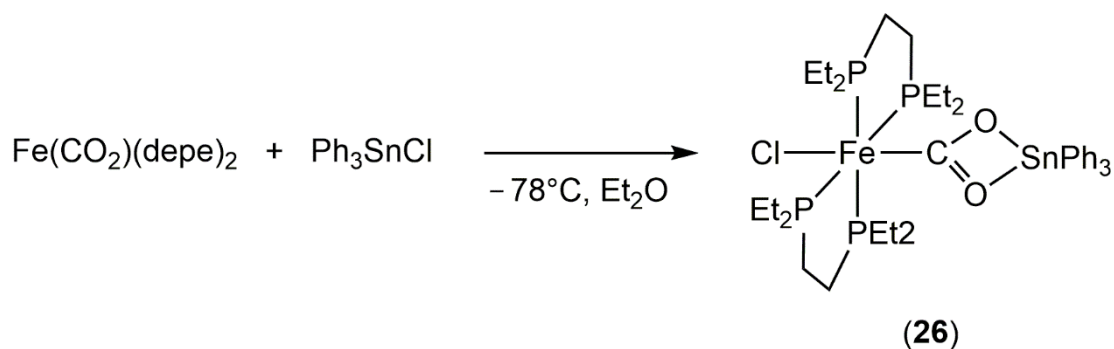


**Figure 24.** Molecular structure of **25**, adapted from [78] (MERCURY view). Hydrogen atoms are omitted for clarity (Sn light blue, O red, N dark blue, Re black, C grey).

In 1997, Komiya et al. reported the synthesis of the  $\text{CO}_2$  complex of iron(0),  $\text{Fe}(\text{CO}_2)(\text{depe})_2$  [depe = 1,2-bis(diethylphosphino)ethane], resulting from the replacement of  $\text{N}_2$  in  $\text{Fe}(\text{N}_2)(\text{depe})_2$  with  $\text{CO}_2$ .  $\text{Fe}(\text{CO}_2)(\text{depe})_2$  reacts then with  $\text{Ph}_3\text{SnCl}$  in  $\text{Et}_2\text{O}$  at  $-78^\circ\text{C}$  to lead to the formation of  $\text{FeCl}(\text{CO}_2\text{SnPh}_3)(\text{depe})_2$  (**26**) (Scheme 26) [79]. The same reaction, using  $\text{Me}_3\text{SnCl}$  as tin precursor, gives rise to the analogous complex  $\text{FeCl}(\text{CO}_2\text{SnMe}_3)(\text{depe})_2$ . The X-ray structure of **26** shows that iron and tin atoms are linked by a  $\text{CO}_2$  molecule, acting as  $\mu(\eta^1\text{-C}:\eta^2\text{-O,O'})$  ligand (Figure 25).



**Scheme 26.** Reaction scheme leading to Compound 26, data from [79].

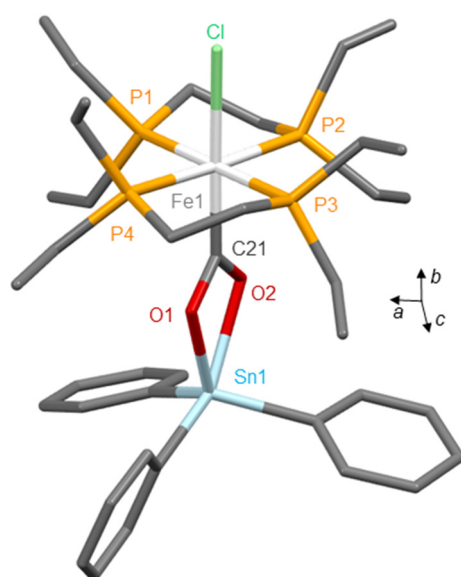


**Figure 25.** Molecular structure of 26, adapted from [79] (MERCURY view). Hydrogen atoms are omitted for clarity (Sn light blue, O red, P orange, Cl light green, Fe white, C grey).

During the last decade, two new metallocarboxylato of tin complexes have been characterized at the solid-state. First of all, in 2011, Adams et al. investigated the reaction of  $\text{Os}_3(\text{CO})_{12}$  with  $\text{Ph}_3\text{SnOH}$  in the presence of  $[\text{Bu}_4\text{N}][\text{OH}]$  in methanol, isolating two new trinuclear osmium clusters characterized as  $\text{Os}_3(\text{CO})_{10}(\mu\text{-}\eta^2\text{-O}=\text{COSnPh}_3)(\mu\text{-O}^-\text{Me})$  (**27**) and  $\text{Os}_3(\text{CO})_{10}(\mu\text{-O}^-\text{Me})(\mu\text{-OH})$  (with yields of 18% and 7%, respectively) [80]. The triphenylgermyl homologue of **27**,  $\text{Os}_3(\text{CO})_{10}(\mu\text{-}\eta^2\text{-O}=\text{COGePh}_3)(\mu\text{-O}^-\text{Me})$ , was also obtained from the reaction of  $\text{Ph}_3\text{GeOH}$  with  $\text{Os}_3(\text{CO})_{12}$  and using a comparable synthetic protocol (in the presence of  $[\text{Bu}_4\text{N}][\text{OH}]$  and in methanol). The authors described the structure of **27** as being a trinuclear cluster of three osmium atoms bearing one bridging methoxy ligand and one bridging triphenylstannylcarboxylate ligand. Remarkably, the Sn–O distances show a large difference in length (2.075 (5) Å and 2.858 (5) Å, respectively), which results from an unusual mode of coordination showing the organotin fragment in a pendant arm arrangement. The carbon atom and one oxygen atom of  $\text{O}=\text{COSnPh}_3$  are bonded to two distinct osmium atoms, while the tin atom is connected via the second oxygen atom of the ligand (Figure 26).

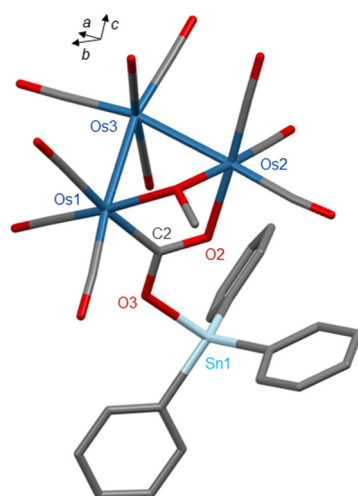


**Figure 26.** Molecular structure of **27**, adapted from [80] (MERCURY view). Hydrogen atoms are omitted for clarity (Sn light blue, O red, Os dark blue, C grey).

Finally, more recently and during investigations devoted to the synthesis and isolation of platinum carbonyl clusters stabilized by Sn(II)-based fragments, Zacchini et al. solved in 2016 the X-ray structure of  $[\text{NEt}_4]_4[\text{Pt}_9(\text{CO})_8(\text{SnCl}_2)_3(\text{SnCl}_3)_2(\text{Cl}_2\text{SnOCOSnCl}_2)] \cdot 2.5\text{CH}_3\text{COCH}_3$  (**28**), which contains an unusual  $[(\text{Cl}_2\text{SnOCOSnCl}_2)]^{2-}$  ligand described as bis-stannyl-carboxylate or carbon dioxide  $\mu_3$ :  $\kappa^3$ -C,O,O'-CO<sub>2</sub> [81]. Cluster **28** was obtained as a side-product from the reaction at room temperature in acetone, involving  $[\text{NEt}_4]_4[\text{Pt}_{15}(\text{CO})_{30}]$ ,  $[\text{NEt}_4]\text{Cl}$  and a large excess of  $\text{SnCl}_2 \cdot 2\text{H}_2\text{O}$ , and leading to the major product  $[\text{NEt}_4]_4[\text{Pt}_6(\text{CO})_6(\text{SnCl}_2)_2(\text{SnCl}_3)_4]$ . The authors described the unprecedented structure of **28** as consisting of a formally neutral Pt<sub>9</sub> core bonded to eight carbonyls, three  $\mu_4$ -SnCl<sub>2</sub>, two  $\mu_3$ -[SnCl<sub>3</sub>]<sup>−</sup> and the six electron donor bis-stannyl-carboxylate  $[(\text{Cl}_2\text{SnOCOSnCl}_2)]^{2-}$  ligand (Figure 27). The possible formation of the metalcarboxylate group is explained by the nucleophilic addition of H<sub>2</sub>O to a terminal CO ligand, followed by deprotonation. Alternatively, the authors also suggest that  $[(\text{Cl}_2\text{SnOCOSnCl}_2)]^{2-}$  could be considered as a carbonite ion  $[\text{CO}_2]^{2-}$  [82], stabilized by coordination at one Pt atom and two Sn atoms. A selection of spectroscopic data (NMR and IR) relating to metalcarboxylato-tin complexes is reported in Table 8.

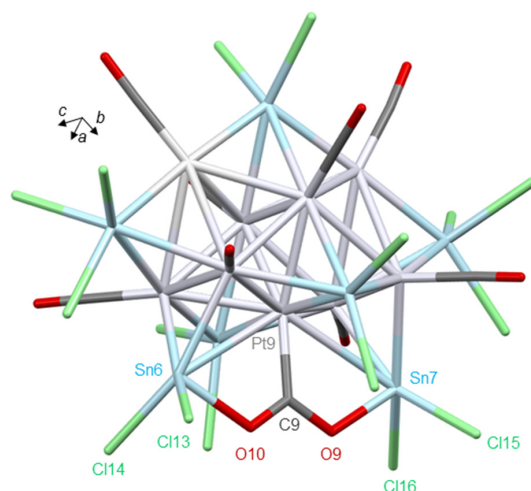


**Figure 27.** Molecular structure of **28**, adapted from [81] (MERCURY view). Hydrogen atoms, two and a half molecules of acetone and four tetra-*n*-butylammonium cations are omitted for clarity (Sn light blue, O red, Cl light green, Pt light grey, C grey).

**Table 7.** Selection of structural parameters found in metallocarboxylato tin complexes.

Compounds	Sn–O(C) (Å)	M–C(O <sub>2</sub> ) (Å)	C–O (Å)	O–C–O (deg)	O–Sn–O (deg)	CSD Entry Deposition Number	Ref.
( $\eta^5$ -C <sub>5</sub> H <sub>5</sub> )Re(NO)(PPh <sub>3</sub> )(CO <sub>2</sub> SnPh <sub>3</sub> ) (16)	2.257(7) 2.175(7)	2.058(9)	1.269(11) 1.313(11)	112.2(8)	57.8(2)	FODLAL 1158240	[72]
( $\eta^5$ -C <sub>5</sub> H <sub>5</sub> )Fe(CO)(PPh <sub>3</sub> )(CO <sub>2</sub> SnPh <sub>3</sub> ) (17)	2.123(4) 2.342(4)	1.931(5)	1.270(6) 1.305(6)	113.4(4)	57.4(1)	JIDLUD 1185927	[73]
( $\eta^5$ -C <sub>9</sub> H <sub>7</sub> )Fe(CO)(PPh <sub>3</sub> )(CO <sub>2</sub> SnPh <sub>3</sub> ) (18)	2.069(2) 2.536(2)	1.933(3)	1.236(3) 1.336(3)	115.9(3)	55.42(7)	HADNUV 1171252	[75]
Cp*Re(CO)(NO)(CO <sub>2</sub> SnPh <sub>3</sub> ) (19)	2.092(3) 2.399(1)	2.100(9)	1.24(1) 1.322(9)	114.6(7)	56.79(5)	YEGCUI 1300837	[76]
CpFe(CO)(PPh <sub>3</sub> )(CO <sub>2</sub> SnMe <sub>3</sub> ) (20)	2.476(3) 2.089(3)	1.936(4)	1.260(6) 1.321(5)	114.3(3)	55.94(9)	YOTBEO 1305570	[77]
CpFe(CO)(PPh <sub>3</sub> )(CO <sub>2</sub> Sn( <i>n</i> -Bu) <sub>3</sub> ) (21)	2.105(4) 2.432(4)	1.934(6)	1.266(7) 1.316(7)	114.2(5)	56.5(1)	YOTBIS 1305571	[77]
Cp*Fe(CO) <sub>2</sub> (CO <sub>2</sub> SnPh <sub>3</sub> ) (22)	2.102(2) 2.394(2)	1.956(3)	1.252(3) 1.312(3)	114.5(2)	56.90(6)	YOTBOY 1305572	[77]
Cp*Re(CO)(NO)(CO <sub>2</sub> SnMe <sub>3</sub> ) (23)	2.054(4) 2.806(4)	2.103(5)	1.237(6) 1.311(6)	117.0(5)	50.3(1)	YOTBUE 1305573	[77]
[Cp*Re(CO)(NO)(CO <sub>2</sub> ) <sub>2</sub> SnMe <sub>2</sub> ] (24)	2.079(6) 2.524(8)	2.11(1)	1.26(1) 1.31(1)	116.8(9)	55.7(2)	NOXRUN 1223123	[78]
Cp*Re(CO)(NO)(CO <sub>2</sub> Sn(Cl)Me <sub>3</sub> ) (25)	2.109(8) 2.287(8)	2.11(1)	1.24(1) 1.32(1)	115.4(9)	58.8(3)	NOXROH	[78]
FeCl(CO <sub>2</sub> SnPh <sub>3</sub> )(depe) <sub>2</sub> (26)	2.097(6) 2.312(7)	1.87(1)	1.28(1) 1.32(1)	108.4(9)	57.0	NOMQIP 1222229	[79]
Os <sub>3</sub> (CO) <sub>10</sub> ( $\mu$ - $\eta^2$ -O=CO <sub>2</sub> SnPh <sub>3</sub> )( $\mu$ -OMe) (27)	2.076(5)	2.080(6)	1.277(8) 1.295(8)	115.6(8)	116.0(4)	IXODAB 807088	[80]
[NEt <sub>4</sub> ] <sub>4</sub> [Pt <sub>9</sub> (CO) <sub>8</sub> (SnCl <sub>2</sub> ) <sub>3</sub> (SnCl <sub>3</sub> ) <sub>2</sub> - (Cl <sub>2</sub> SnOCOSnCl <sub>2</sub> )]·2.5CH <sub>3</sub> COCH <sub>3</sub> (28)	2.088(9) 2.122(9)	2.03(1)	1.28(1) 1.31(2)	116(1)	115.5(7) 117.8(8)	KAKLOA 1439435	[81]

**Table 8.** Selection of spectroscopic data (NMR and IR) assigned to metallocarboxylato tin complexes.

Compounds	<sup>119</sup> Sn{ <sup>1</sup> H} NMR ( $\delta$ , ppm)	<sup>13</sup> C{ <sup>1</sup> H} NMR M–CO <sub>2</sub> ( $\delta$ , ppm)	IR $\nu$ (OCO) (cm <sup>-1</sup> )	Ref.
( $\eta^5$ -C <sub>5</sub> H <sub>5</sub> )Re(NO)(PPh <sub>3</sub> )(CO <sub>2</sub> SnPh <sub>3</sub> ) (16)	−167.1 <sup>a</sup> $J_{119\text{Sn},31\text{P}} = 4.6$ Hz	207.6 <sup>a</sup>	1395, 1188	[72]
Cp*Re(CO)(NO)(CO <sub>2</sub> SnPh <sub>3</sub> ) (19)	na	206.94 <sup>b</sup>	1429, 1174	[76]
CpFe(CO)(PPh <sub>3</sub> )(CO <sub>2</sub> SnMe <sub>3</sub> ) (20)	na	219.63 <sup>a</sup> d, $J_{\text{P,C}} = 30.2$ Hz 220.42 <sup>c</sup> d, $J_{\text{P,C}} = 32.5$ Hz	1433, 1132	[77]
CpFe(CO)(PPh <sub>3</sub> )(CO <sub>2</sub> Sn( <i>n</i> -Bu) <sub>3</sub> ) (21)	na	219.56 <sup>a</sup> d, $J_{\text{P,C}} = 30.9$ Hz 220.29 <sup>c</sup> d, $J_{\text{P,C}} = 31.4$ Hz	1480, 1132	[77]
Cp*Fe(CO) <sub>2</sub> (CO <sub>2</sub> SnPh <sub>3</sub> ) (22)	na	215.10 <sup>a</sup>	1470, 1146	[77]
Cp*Re(CO)(NO)(CO <sub>2</sub> SnMe <sub>3</sub> ) (23)	na	197.58 <sup>a</sup> 196.10 <sup>c</sup>	1512, 1162	[77]
Cp*Re(CO)(NO)(CO <sub>2</sub> Sn(Cl)Me <sub>2</sub> ) (24)	na	205.66 <sup>d</sup>	1385, 1246	[78]
[Cp*Re(CO)(NO)(CO <sub>2</sub> ) <sub>2</sub> SnMe <sub>2</sub> ] (25)	na	202.14 <sup>d</sup>	1469, 1186	[78]
FeCl(CO <sub>2</sub> SnPh <sub>3</sub> )(depe) <sub>2</sub> (26)	na	243.8 <sup>d</sup> qui, $J_{\text{P,C}} = 22$ Hz	1306	[80]

<sup>a</sup> Measured in chloroform-d; <sup>b</sup> methylenchloride-d<sub>2</sub>; <sup>c</sup> measured in tetrahydrofuran-d<sub>8</sub>; <sup>d</sup> measured in benzene-d<sub>6</sub>.

## 6. Conclusions

In the conclusion of the first part of this inventory, “CO<sub>2</sub> Derivatives of Molecular Tin Compounds. Part 1: Hemicarbonato and Carbonato Complexes”, we previously claimed that the CO<sub>2</sub> derivatives of molecular tin compounds could truly be considered as a class of compounds in their own right. The additional solid-state structures described in this second part and focusing more specifically on carbamato, formato, phosphinoformato and metallocarboxylato complexes, contribute assuredly to reinforce this point of view. Once again, a rich diversity of architectures, including discrete, dimeric, polynuclear and polymeric structures, and exhibiting various modes of coordination, sometimes totally

unusual, were highlighted. Thus, this collection of compounds supports again the great reactivity of molecular tin complexes toward carbon dioxide and underlines the facile insertion of CO<sub>2</sub> into Sn–X bonds (X = OR, N, H, P). This reactivity, which has been known for a long time, has already been efficiently used for catalytic applications involving CO<sub>2</sub> and organotins, in particular as has been shown, with the aim of accessing carbamate compounds and their derivatives. However, the latest advances recently published are very interesting and promising, suggesting new perspectives in terms of reactivity of organotins with respect to small molecules and in particular for the activation of carbon dioxide. This is especially the case of studies relating to the reductive hydroboration of CO<sub>2</sub> or those involving the formation of CO<sub>2</sub>-Sn/phosphorus frustrated Lewis pairs (FLP) adducts, which start new insights. In the field of inorganic chemistry, the isolation of a new cluster incorporating a bis-stannyl-carboxylate group, also viewed as the coordination of a carbonite fragment, constitutes an innovative result which can be considered as unprecedented. Thus, the second half of the last century was incontestably a period of strong developments and fundamental advances in organotin chemistry, but the coming decades promise to be just as fruitful and exciting in terms of progress and inventiveness, and in particular, in the quest to activate carbon dioxide.

**Funding:** The author thanks the Centre National de la Recherche Scientifique (C.N.R.S-France) and the University of Bourgogne Franche-Comté for financial support.

**Institutional Review Board Statement:** Not applicable.

**Informed Consent Statement:** Not applicable.

**Data Availability Statement:** Not applicable.

**Acknowledgments:** A special thanks to three anonymous reviewers for their judicious corrections and suggestions which have contributed to improving the manuscript.

**Conflicts of Interest:** The author declares no conflict of interest.

## References

1. Plasseraud, L. CO<sub>2</sub> derivatives of molecular tin compounds. Part 1: Hemicarbonato and carbonato complexes. *Inorganics* **2020**, *8*, 31. [\[CrossRef\]](#)
2. Aresta, M.; Nobile, C.F.; Albano, V.G.; Forni, E.; Manassero, M. New nickel-carbon dioxide complex: Synthesis, properties, and crystallographic characterization of (carbon dioxide)bis(tricyclohexylphosphine)nickel. *J. Chem. Soc. Chem. Commun.* **1975**, 636–637. [\[CrossRef\]](#)
3. Álvarez, M.; Galindo, A.; Pérez, P.J.; Carmona, E. Molybdenum and tungsten complexes with carbon dioxide and ethylene ligands. *Chem. Sci.* **2019**, *10*, 8541–8546. [\[CrossRef\]](#)
4. Gibson, D.H. The organometallic chemistry of carbon dioxide. *Chem. Rev.* **1996**, *96*, 2063–2096. [\[CrossRef\]](#) [\[PubMed\]](#)
5. Mascetti, J. Carbon dioxide coordination chemistry and reactivity of coordinated CO<sub>2</sub>. In *Carbon Dioxide as Chemical Feedstock*; Aresta, M., Ed.; Wiley-VCH Verlag GmbH & Co. KGaA: Weinheim, Germany, 2010; pp. 55–88.
6. Mascetti, J. Metal coordination of CO<sub>2</sub>. In *Encyclopedia of Inorganic and Bioinorganic Chemistry*; Wiley: Hoboken, NJ, USA, 2014; pp. 1–17.
7. Aresta, M.; Dibenedetto, A.; Quaranta, E. CO<sub>2</sub> coordination to metal centres: Modes of bonding and reactivity. In *Reaction Mechanisms in Carbon Dioxide Conversion*; Springer: Berlin/Heidelberg, Germany, 2016; pp. 35–69.
8. Paparo, A.; Okuda, J. Carbon dioxide complexes: Bonding modes and synthetic methods. *Coord. Chem. Rev.* **2017**, *334*, 136–149. [\[CrossRef\]](#)
9. Holscher, M.; Gurtler, C.; Keim, W.; Muller, T.E.; Peters, M.; Leitner, W. Carbon dioxide as a carbon resource—Recent trends and perspectives. *Z. Naturforschung B* **2012**, *67b*, 961–975. [\[CrossRef\]](#)
10. Dibenedetto, A.; Angelini, A.; Stufano, P. Use of carbon dioxide as feedstock for chemicals and fuels: Homogeneous and heterogeneous catalysis. *J. Chem. Tech. Biotech.* **2014**, *89*, 334–353. [\[CrossRef\]](#)
11. Wang, H.; Gao, P.; Zhao, T.; Wei, W.; Sun, Y. Recent advances in the catalytic conversion of CO<sub>2</sub> to value added compounds. *Sci. China Chem.* **2015**, *58*, 79–92. [\[CrossRef\]](#)
12. Liu, Q.; Wu, L.; Jackstell, R.; Beller, M. Using carbon dioxide as a building block in organic synthesis. *Nat. Commun.* **2015**, *6*, 5933. [\[CrossRef\]](#) [\[PubMed\]](#)
13. Kleij, A.W.; North, M.; Urakawa, A. CO<sub>2</sub> catalysis. *ChemSusChem* **2017**, *10*, 1036–1038. [\[CrossRef\]](#)
14. Dabral, S.; Schaub, T. The use of carbon dioxide (CO<sub>2</sub>) as a building block in organic synthesis from an industrial perspective. *Adv. Synth. Catal.* **2019**, *361*, 223–246. [\[CrossRef\]](#)

15. Jana, A.; Tavčar, G.; Roesky, H.W.; John, M. Germanium(II) hydride mediated reduction of carbon dioxide to formic acid and methanol with ammonia borane as the hydrogen source. *Dalton Trans.* **2010**, *39*, 9487–9489. [[CrossRef](#)]
16. Villegas-Escobar, N.; Schaefer, H.F., III; Toro-Labbé, A. Formation of formic acid derivatives through activation and hydroboration of CO<sub>2</sub> by low-valent group 14 (Si, Ge, Sn, Pb) catalysts. *J. Phys. Chem. A* **2020**, *124*, 1121–1133. [[CrossRef](#)]
17. Groom, C.R.; Bruno, I.J.; Lightfoot, S.C.; Ward, S.C. The Cambridge Structural Database. *Acta Cryst.* **2016**, *B72*, 171–179. [[CrossRef](#)] [[PubMed](#)]
18. Wang, H.; Xin, Z.; Li, Y. Synthesis of ureas from CO<sub>2</sub>. *Top. Curr. Chem.* **2017**, *375*, 1–26.
19. Yang, Z.-Z.; He, L.-N.; Gao, J.; Liu, A.-H.; Yu, B. Carbon dioxide utilization with C–N bond formation: Carbon dioxide capture and subsequent conversion. *Energy Environ. Sci.* **2012**, *5*, 6602–6639. [[CrossRef](#)]
20. Li, J.-Y.; Song, Q.-W.; Zhang, K.; Liu, P. Catalytic conversion of carbon dioxide through C–N bond formation. *Molecules* **2019**, *24*, 182. [[CrossRef](#)]
21. Dalpozzo, R.; Della Ca', N.; Gabriele, B.; Mancuso, R. Recent advances in the chemical fixation of carbon dioxide: A green route to carbonylated heterocycle synthesis. *Catalysts* **2019**, *9*, 511. [[CrossRef](#)]
22. Tominaga, K.-I.; Sasaki, Y. Synthesis of 2-oxazolidinones from CO<sub>2</sub> and 1,2-aminoalcohols catalyzed by *n*-Bu<sub>2</sub>SnO. *Synlett* **2002**, *2*, 307–309. [[CrossRef](#)]
23. Pulla, S.; Felton, C.M.; Gartia, Y.; Ramidi, P.; Ghosh, A. Synthesis of 2-oxazolidinones by direct condensation of 2-aminoalcohols with carbon dioxide using chlorostannoxanes. *ACS Sustain. Chem. Eng.* **2013**, *1*, 309–312. [[CrossRef](#)]
24. Chaturvedi, D. Perspectives on the synthesis of organic carbamates. *Tetrahedron* **2012**, *68*, 15–45. [[CrossRef](#)]
25. Dell'Amico, D.B.; Calderazzo, F.; Labella, L.; Marchetti, F.; Pampaloni, G. Converting carbon dioxide into Carbamate Derivatives. *Chem. Rev.* **2003**, *103*, 3857–3898. [[CrossRef](#)]
26. Bresciani, G.; Biancalana, L.; Pampaloni, G.; Marchetti, F. Recent advances in the chemistry of metal carbamates. *Molecules* **2020**, *25*, 3603. [[CrossRef](#)]
27. Zhu, G.; Li, H.; Cao, Y.; Liu, H.; Li, X.; Chen, J.; Tang, Q. Kinetic study on the novel efficient clean decomposition of methyl *N*-phenyl carbamate to phenyl isocyanate. *Ind. Eng. Chem. Res.* **2013**, *52*, 4450–4454. [[CrossRef](#)]
28. Heyn, R.H.; Jacobs, I.; Carr, R.H. Chapter three—Synthesis of aromatic carbamates from CO<sub>2</sub>: Implications for the polyurethane industry. *Adv. Inorg. Chem.* **2014**, *66*, 83–115.
29. Abila, M.; Choi, J.-C.; Sakakura, T. Halogen-free process for the conversion of carbon dioxide to urethanes by homogeneous catalysis. *Chem. Commun.* **2001**, 2238–2239. [[CrossRef](#)] [[PubMed](#)]
30. Yuan, H.-Y.; Choi, J.-C.; Onozawa, S.-y.; Fukaya, N.; Choi, S.J.; Yasuda, H.; Sakakura, T. The direct synthesis of *N*-phenylcarbamates from CO<sub>2</sub>, aniline, and dibutyltin dialkoxide. *J. CO<sub>2</sub> Util.* **2016**, *16*, 282–286. [[CrossRef](#)]
31. Ballivet-Tkatchenko, D.; Chermette, H.; Plasseraud, L.; Walter, O. Insertion reaction of carbon dioxide into Sn–OR bond. Synthesis, structure and DFT calculations of di- and tetranuclear isopropylcarbonato tin(IV) complexes. *Dalton Trans.* **2006**, 5167–5175. [[CrossRef](#)] [[PubMed](#)]
32. Germain, N.; Müller, I.; Hanauer, M.; Paciello, R.A.; Baumann, R.; Trapp, O.; Schaub, T. Synthesis of industrially relevant carbamates towards isocyanates using carbon dioxide and organotin(IV) alkoxides. *ChemSusChem* **2016**, *9*, 1586–1590. [[CrossRef](#)] [[PubMed](#)]
33. Germain, N.; Hermsen, M.; Schaub, T.; Trapp, O. Synthesis of carbamates from carbon dioxide promoted by organostannanes and alkoxy silanes. *Appl. Organomet. Chem.* **2017**, *31*, e3733. [[CrossRef](#)]
34. Ballivet-Tkatchenko, D.; Jerphagnon, T.; Ligabue, R.; Plasseraud, L.; Poinot, D. The role of distannoxanes in the synthesis of dimethyl carbonate from carbon dioxide. *Appl. Catal. Gen.* **2003**, *255*, 93–99. [[CrossRef](#)]
35. Bloodworth, A.J.; Davies, A.G. Organometallic reactions. Part I. The addition of tin alkoxides to isocyanates. *J. Chem. Soc.* **1965**, 5238–5244. [[CrossRef](#)]
36. Bloodworth, A.J.; Davies, A.G. Organometallic reactions. Part II. The addition of bistrialkyltin oxides to isocyanates. *J. Chem. Soc.* **1965**, 6245–6249. [[CrossRef](#)]
37. Harrison, P.G.; Zuckerman, J.J. Structural studies in main group chemistry III. Tin-119m Mössbauer investigation of some tin-nitrogen bonded compounds. *J. Organomet. Chem.* **1973**, *55*, 261–266. [[CrossRef](#)]
38. Devendra, R.; Edmonds, N.R.; Söhnel, T. Interaction between trialkyltin alkoxide and phenyl isocyanate in the formation of tin carbamate: A computational and experimental study. *J. Mol. Catal. A* **2014**, *395*, 72–86. [[CrossRef](#)]
39. Bloodworth, A.J.; Davies, A.G.; Vasishtha, S.C. Organometallic reactions. Part XIV. The decarboxylation of trialkyltin carbamates by isocyanates and isothiocyanates: A new route to carbodi-imides. *J. Chem. Soc. C* **1968**, 2640–2646. [[CrossRef](#)]
40. Shibata, I.; Yamasaki, H.; Baba, A.; Matsuda, H. A novel Darzens-type reaction promoted by tributylstannylcarbamate. *J. Org. Chem.* **1992**, *57*, 6909–6914. [[CrossRef](#)]
41. Shibata, I.; Mori, Y.; Yamasaki, H.; Baba, A.; Matsuda, H. Novel Michael addition promoted by tributylstannylcarbamate. Synthesis of diacyclicpropanes. *Tetrahedron Lett.* **1993**, *34*, 6567–6570. [[CrossRef](#)]
42. Zakharov, N.; Struchkov, Y.T.; Ganina, V.I.; Kuz'min, E.A. X-ray crystallographic investigation of nonbinding interactions and coordination in organometallic compounds. XV. The crystal structure of the trimethylstannyl ester of trimethylstannylcarbamate Me<sub>3</sub>SnNHC(=O)–OSnMe<sub>3</sub>. *Zhurnal Strukturnoi Khimii* **1980**, *21*, 162–167.
43. Plasseraud, L. Organotin(IV) complexes containing Sn–O–Se moieties: A structural inventory. *Synthesis* **2018**, *50*, 3653–3661. [[CrossRef](#)]

44. Kümmerlen, J.; Sebald, A.; Reuter, H. The structure of  $(^i\text{Bu}_3\text{Sn})_2\text{CO}_3$  and  $(\text{Me}_3\text{Sn})_2\text{CO}_3$  in solution and in the solid state studied by  $^{13}\text{C}/^{119}\text{Sn}$  NMR spectroscopy and X-ray diffraction. *J. Organomet. Chem.* **1992**, *427*, 309–323. [[CrossRef](#)]
45. Abis, L.; Belli Dell'Amico, D.; Calderazzo, F.; Caminiti, R.; Garbassi, F.; Ianelli, S.; Pelizzi, G.; Robino, P.; Tomei, A. *N,N*-Dialkylcarbamato complexes as precursors for the chemical implantation of metal cations on a silica support. Part I. Tin. *J. Mol. Catal. Chem.* **1996**, *108*, L113–L117. [[CrossRef](#)]
46. Horley, G.A.; Mahon, M.F.; Molloy, K.C. Synthesis and characterization of novel homoleptic *N,N*-dialkylcarbamato complexes of antimony: Precursors for the deposition of antimony oxides. *Inorg. Chem.* **2002**, *41*, 5052–5058. [[CrossRef](#)] [[PubMed](#)]
47. Komarov, N.V.; Ryzhkova, N.A.; Andreev, A.A. Synthesis of alkoxytannanes by reactions of *O*-(organylstannyl) carbamates with alcohols. *Russ. Chem. Bull.* **2004**, *53*, 936–938. [[CrossRef](#)]
48. Levashov, A.S.; Andreev, A.A.; Buryi, D.S.; Konshin, V.V. A reaction of tin tetra(*N,N*-diethylcarbamate) with phenylacetylene as a new route to tetra(phenylethynyl)tin. *Russ. Chem. Bull.* **2015**, *63*, 775–776. [[CrossRef](#)]
49. Buryi, D.S.; Levashov, A.S. The reaction of tin tetracarbamates with organyl chlorosilanes: A novel synthetic route towards *O*-silylurethanes. *Russ. J. Gen. Chem.* **2019**, *89*, 924–928. [[CrossRef](#)]
50. Stewart, C.A.; Dickie, D.A.; Parkes, M.V.; Saria, J.A.; Kemp, R.A. Reactivity of bis(2,2,5,5-tetramethyl-2,5-disila-1-azacyclopent-1-yl)tin with  $\text{CO}_2$ , OCS, and  $\text{CS}_2$  and comparison to that of bis[bis(trimethylsilyl)amido]tin. *Inorg. Chem.* **2010**, *49*, 11133–11141. [[CrossRef](#)]
51. Sita, L.R.; Babcock, J.R.; Xi, R. Facile metathetical exchange between carbon dioxide and the divalent group 14 bisamides  $\text{M}[\text{N}(\text{SiMe}_3)_2]_2$  ( $\text{M} = \text{Ge}$  and  $\text{Sn}$ ). *J. Am. Chem. Soc.* **1996**, *118*, 10912–10913. [[CrossRef](#)]
52. Stewart, C.A.; Dickie, D.A.; Tang, Y.; Kemp, R.A. Insertion reactions of  $\text{CO}_2$ , OCS, and  $\text{CS}_2$  into the  $\text{Sn}-\text{N}$  bonds of  $(\text{Me}_2\text{N})_2\text{Sn}$ : NMR and X-ray structural characterization of the products. *Inorg. Chim. Acta* **2011**, *376*, 73–79. [[CrossRef](#)]
53. Harris, L.A.-M.; Coles, M.P.; Fulton, J.R. Synthesis and reactivity of tin amide complexes. *Inorg. Chim. Acta* **2011**, *369*, 97–102. [[CrossRef](#)]
54. Elöd, E.; Kolbach, F. Tin salts of organic acids. *Z. Anorganische Allgemeine Chem.* **1927**, *164*, 297–312. [[CrossRef](#)]
55. Donaldson, J.D.; Knifton, J.F. Complex tin(II) formates. *J. Chem. Soc.* **1964**, 6107–6113. [[CrossRef](#)]
56. Jelen, A.; Lindqvist, O. The crystal structure of potassium triformatostannate(II),  $\text{KSn}(\text{HCOO})_3$ . *Acta Chem. Scand.* **1969**, *23*, 3071–3080. [[CrossRef](#)]
57. Harrison, P.G.; Thornton, E.W. Derivatives of bivalent germanium, tin, and lead. Part 21. Tin(II) formate: A reinvestigation. *J. C. S. Dalton* **1978**, 1274–1278. [[CrossRef](#)]
58. Molloy, K.C.; Quill, K.; Nowell, I.W. Organotin biocides. Part 8. The crystal structure of triphenyltin formate and a comparative variable-temperature tin-119 Mössbauer spectroscopic study of organotin formates and acetates. *J. Chem. Soc. Dalton Trans.* **1987**, 101–106. [[CrossRef](#)]
59. Mistry, F.; Rettig, S.J.; Trotter, J.; Aubke, F. Structure of bis(formato)dimethyltin(IV). *Acta Cryst.* **1990**, *C46*, 2091–2093. [[CrossRef](#)]
60. Ellis, B.D.; Atkins, T.M.; Peng, Y.; Sutton, A.D.; Gordon, J.C.; Power, P.P. Synthesis and thermolytic behavior of tin(IV) formates: In search of recyclable metal-hydride systems. *Dalton Trans.* **2010**, *39*, 10659–10663. [[CrossRef](#)] [[PubMed](#)]
61. McMurtrie, J.C.; Arnorld, D.P. Tin(IV) porphyrin complexes. Crystal structures of *meso*-tetraphenyl-porphyrinatotin(IV) diacetate, *bis*(dichloro-acetate), *bis*(trifluoroacetate) and diformate, and structural correlations for tin(IV) porphyrin complexes with *O*-bound anionic ligands. *J. Struct. Chem.* **2010**, *51*, 107–113. [[CrossRef](#)]
62. Jana, A.; Roesky, H.W.; Schulzke, C.; Döring, A. Reactions of tin(II) hydride species with unsaturated molecules. *Angew. Chem. Int. Ed.* **2009**, *48*, 1106–1109. [[CrossRef](#)] [[PubMed](#)]
63. Albertin, G.; Antoniutti, S.; Castro, J.; García-Fontán, S.; Zanardo, G. Preparation and reactivity of stannyl complexes of manganese and rhenium. *Organometallics* **2007**, *26*, 2918–2930. [[CrossRef](#)]
64. Albertin, G.; Antoniutti, S.; Bacchi, A.; Pelizzi, G.; Zanardo, G. Synthesis and reactivity of trihydridostannyl complexes of ruthenium and osmium. *Organometallics* **2008**, *27*, 4407–4418. [[CrossRef](#)]
65. Albertin, G.; Antoniutti, S.; Castro, J. Reactivity of dihydrides  $\text{MH}_2\text{P}_4$  ( $\text{M} = \text{Fe}$ ,  $\text{Ru}$ ,  $\text{Os}$ ) with  $\text{SnCl}_2$ : Preparation of bis(trihydridestannyl) derivatives. *Organometallics* **2010**, *29*, 3808–3816. [[CrossRef](#)]
66. Otte, F.; Koller, S.G.; Golz, C.; Strohmman, C. Crystal structures of diaquadi- $\mu$ -hydroxido-tris[trimethyltin(IV)] diformatotrimethylstannate(IV) and di- $\mu$ -hydroxido-tris[trimethyltin(IV)] chloride monohydrate. *Acta Cryst.* **2016**, *E72*, 1499–1502. [[CrossRef](#)]
67. Hadlington, T.J.; Kefalidis, C.E.; Maron, L.; Jones, C. Efficient reduction of carbon dioxide to methanol equivalents catalyzed by two-coordinate amido-germanium(II) and -tin(II) hydride complexes. *ACS Catal.* **2017**, *7*, 1853–1859. [[CrossRef](#)]
68. Zhu, C.; Frigge, R.; Turner, A.M.; Kaiser, R.I.; Sun, B.-J.; Chen, S.-Y.; Chang, A.H.H. First identification of unstable phosphino formic acid ( $\text{H}_2\text{PCOOH}$ ). *Chem. Commun.* **2018**, *54*, 5716–5719. [[CrossRef](#)]
69. Dickie, D.A.; Coker, E.N.; Kemp, R.A. Formation of a reversible, intramolecular main-group metal- $\text{CO}_2$  adduct. *Inorg. Chem.* **2011**, *50*, 11288–11290. [[CrossRef](#)]
70. Holtkamp, P.; Friedrich, F.; Stratmann, E.; Mix, A.; Neumann, B.; Stammeler, H.-G.; Mitzel, N.W. A neutral germinal tin/phosphorus frustrated Lewis pair. *Angew. Chem. Int. Ed.* **2019**, *58*, 5114–5118. [[CrossRef](#)] [[PubMed](#)]
71. Pinkes, J.R.; Cutler, A.R. Iron-tin carbon dioxide complexes ( $\eta^5\text{-C}_5\text{Me}_5$ )( $\text{CO}$ ) $_2\text{Fe-CO}_2\text{SnR}_3$  ( $\text{R} = \text{Me}$ ,  $\text{Ph}$ ): Observations pertaining to unsymmetrical metalcarboxylates and carboxylate-carbonyl  $^{13}\text{C}$ -label exchange. *Inorg. Chem.* **1994**, *33*, 759–764. [[CrossRef](#)]

72. Senn, D.R.; Gladysz, J.A.; Emerson, K.; Larsen, R.D. Synthesis, structure, and reactivity of transition-metal/main-group-metal bridging carboxylate complexes of the formula  $(\eta^5\text{-C}_5\text{H}_5)\text{Re}(\text{NO})(\text{PPh}_3)(\text{CO}_2\text{ML}_n)$  ( $\text{M} = \text{Li}, \text{K}, \text{Ge}, \text{Sn}, \text{Pb}$ ). *Inorg. Chem.* **1987**, *26*, 2737–2739. [[CrossRef](#)]
73. Gibson, D.H.; Richardson, J.F.; Ong, T.-S. 1-Carbonyl-1- $\eta^5$ -cyclopentadienyl-2,2,2-triphenyl-1-triphenylphosphine- $\mu$ -carboxylato-1 $\kappa\text{C}$ :2 $\kappa\text{O}$ :2 $\kappa\text{O}'$ -irontin. *Acta Cryst.* **1991**, *C47*, 259–261. [[CrossRef](#)]
74. Holmes, R.R.; Day, R.O.; Chandrasekhar, V.; Vollano, J.F.; Holmes, J.M. Pentacoordinated molecules. 65. Discrete, dimeric, and polymeric structures of triphenyltin esters of chlorobenzoic acids. *Inorg. Chem.* **1986**, *25*, 2490–2494. [[CrossRef](#)]
75. Gibson, D.H.; Richardson, J.F.; Mbadike, O.P. 1-Carbonyl- $\mu$ -carboxylato-1 $\kappa\text{C}$ :2 $\kappa\text{O}$ :2 $\kappa\text{O}'$ -1- $\eta^5$ -indenyl-2,2,2-triphenyl-1-(triphenylphosphine)irontin. *Acta Cryst.* **1993**, *B49*, 784–786. [[CrossRef](#)]
76. Gibson, D.H.; Mehta, J.M.; Ye, M.; Richardson, J.F.; Mashuta, M.S. Synthesis and characterization of rhenium metallocarboxylates. *Organometallics* **1994**, *13*, 1070–1072. [[CrossRef](#)]
77. Gibson, D.H.; Ye, M.; Sleadd, B.A.; Mehta, J.M.; Mbadike, O.P.; Richardson, J.F.; Mashuta, M.S. Characterization and thermolysis reactions of  $\text{CO}_2$ -bridged iron-tin and rhenium-tin complexes. Structure-reactivity correlations. *Organometallics* **1995**, *14*, 1242–1255. [[CrossRef](#)]
78. Gibson, D.H.; Mehta, J.M.; Mashuta, M.S.; Richardson, J.F. Synthesis and characterization of new rhenium—Tin complexes with  $\mu_2$ - $\eta^3$ -bridging  $\text{CO}_2$  ligands. *Organometallics* **1997**, *16*, 4828–4832. [[CrossRef](#)]
79. Hirano, M.; Akita, M.; Tani, K.; Kumagai, K.; Kasuga, N.C.; Fukuoka, A.; Komiya, S. Activation of coordinated carbon dioxide in  $\text{Fe}(\text{CO})_2(\text{depe})_2$  by group 14 Electrophiles. *Organometallics* **1997**, *16*, 4206–4213. [[CrossRef](#)]
80. Adams, R.D.; Chen, M.; Trufan, E. Complexes containing bridging tin- and germanium-substituted metallocarboxylate ligands from the reactions of  $\text{Ph}_3\text{SnOH}$  and  $\text{Ph}_3\text{GeOH}$  with  $\text{Os}_3(\text{CO})_{12}$  in the presence of base. *J. Organomet. Chem.* **2011**, *696*, 2894–2898. [[CrossRef](#)]
81. Bortoluzzi, M.; Ceriotti, A.; Ciabatti, I.; Della Pergola, R.; Femoni, C.; Iapalucci, M.C.; Storione, A.; Zacchini, S. Platinum carbonyl clusters stabilized by Sn(II)-based fragments: Syntheses and structures of  $[\text{Pt}_6(\text{CO})_6(\text{SnCl}_2)_2(\text{SnCl}_3)_4]^{4-}$ ,  $[\text{Pt}_9(\text{CO})_8(\text{SnCl}_2)_3(\text{SnCl}_3)_2(\text{Cl}_2\text{SnOCOSnCl}_2)]^{4-}$  and  $[\text{Pt}_{10}(\text{CO})_{14}(\text{Cl}_2\text{Sn}(\text{OH})\text{SnCl}_2)_2]^{2-}$ . *Dalton Trans.* **2016**, *45*, 5001–5013. [[CrossRef](#)] [[PubMed](#)]
82. Paparo, A.; Okuda, J. Carbonite, the dianion of carbon dioxide and its metal complexes. *J. Organomet. Chem.* **2018**, *869*, 270–274. [[CrossRef](#)]